A SET OF SHELL FINITE ELEMENTS FOR DYNAMIC ANALYSIS OF COOLING TOWERS

Prepared by

T.Y. Yang and Rakesh K. Kapania
School of Aeronautics and Astronautics
Purdue University
West Lafayette, Indiana 47907

Submitted to

THE NATIONAL SCIENCE FOUNDATION

June 10, 1982

50272-101

REPORT DOCUMENTATION PAGE	1. REPORT NO. NSF/CEE-82026	2.	3. Recipient's Accession No. PB83-100990
4. Title and Subtitle: Set of Shell Finite elements for Dynamic Analysis of Cooling Towers			5. Report Date: June 1982 6.
7. Author(s): T.Y. Yang, R.K. Kapania			8. Performing Organization Rept. No.
9. Performing Organization Name and Address: Purdue University School of Aeronautics and Astronautics West Lafayette, IN 47907			10. Project/Task/Work Unit No. 11. Contract(C) or Grant(G) No. (C) (G) CEE8024883
12. Sponsoring Organization Name and Address: Directorate for Engineering (ENG) National Science Foundation 1800 G Street, N.W. Washington, DC 20550			13. Type of Report & Period Covered 14.

15. Supplementary Notes
Submitted by: Communications Program (OPRM)
National Science Foundation
Washington, DC 20550

16. Abstract (Limit: 200 words)

A set of shell finite elements is adopted, modified, or extended to study the dynamic responses of complex, thin shell structures and column-supported cooling towers due to earthquake excitation and wind loads. The elements are formulated to achieve optimum finite element modeling of the column-supported cooling towers according to the distributions of dominating bending and membrane stresses, and to model the vulnerable shell column region using discrete column elements and quadrilateral shell shell elements. Examples are provided to evaluate a single type, combined types, and the whole set of elements. The whole set of elements is used to determine the first three eccentric natural frequencies of a column-supported cooling tower. The mean stresses and displacements in a fixed base cooling tower are determined and the results are found to be in excellent agreement with the known alternative solutions.

17. Document Analysis a. Descriptors

Structural analysis
Dynamic structural analysis
Earthquakes
Cooling towers
Shell structures
Thin shell structures
Mathematical models
Loads (forces)
Stresses
Displacement

b. Identifiers/Open-Ended Terms

Matrix methods
T.Y. Yang, /PI

c. COSATI Field/Group

18. Availability Statement	19. Security Class (This Report)	21. No. of Pages
NTIS	20. Security Class (This Page)	22. Price

ACKNOWLEDGMENTS

This study is sponsored by the National Science Foundation under Grant #CEE-8024883. The authors gratefully acknowledge Dr. S.C. Liu of NSF for his technical guidance. Dr. S.C. Liu is the program manager for year one and Dr. Michael P. Gaus will be the program manager for year two. The project period is from 6/1/81 to 5/31/83.

The authors also wish to acknowledge the Co-principal Investigator Professor Y.K. Lin of the University of Illinois at Urbana-Champaign and Professor Anshel J. Schiff of Purdue University for their technical advices. Mr. Sunil Saigal, another research assistant to this project, has provided assistance through technical discussions.

TABLE OF CONTENTS

Page

LIST OF TABLES

LIST OF FIGURES

ABSTRACT

A set of shell finite elements is adopted, modified or extended to study the dynamic responses of complex thin shell structures in general, and column supported cooling towers in particular, due to earthquake excitation and wind loads. The elements are formulated intending to achieve optimum finite element modeling of the column-supported cooling towers according to the distributions of dominating bending and membrane stresses and intending to model the vulnerable shell-column region using discrete column elements and quadrilateral shell elements. The set includes: a 16 d.o.f. column element; a 48 d.o.f. doubly-curved quadrilateral general shell element; a 42 d.o.f. doubly-curved general-membrane transition element; a 21 d.o.f. and a 39 d.o.f. doubly-curved triangular membrane filter element; and a 28 d.o.f. doubly-curved quadrilateral membrane element.

Examples are illustrated to evaluate a single type, combined types and the whole set of elements. The 48 d.o.f. high-order quadrilateral curved shell element is employed to analyze: (1) a fixed base cooling tower subjected to its own weight; (2) an orthotropic cylindrical shell with both edges clamped subjected to internal pressure; (3) axisymmetric free vibrations of a spherical cap with base clamped; (4) axisymmetric buckling of a simply-supported cylinderical shell subjected to axial compression; and (5) free vibration analysis of a fixed base cooling tower with and without initial stresses. The 42 d.o.f. general-membrane transition element is tested by employing it in conjunction with the general 48 d.o.f. element and an existing 28 d.o.f. high-precision membrane element to determine the first eccentric natural frequency of a fixed

base cooling tower. The 21 d.o.f. and the 39 d.o.f. membrane triangular 'filler' elements are evaluated through their performance on two examples: (1) axisymmetric free vibration of a spherical membrane cap with base on "rollers"; and (2) first eccentric natural frequency of a fixed base cooling tower.

The whole set of elements is then employed to determine the first three eccentric natural frequencies of a column-supported cooling tower.

The mean stresses and displacements in a fixed base cooling tower due to a wind velocity of 29 ft/sec. and assuming Batch and Hopley pressure distribution along the circumference are also determined using the 48 d.o.f. general shell element. All results are found to be in excellent agreement with the known alternative solutions.

The modeling may be used in seismic response analysis of cooling towers for obtaining detail stress distribution in the vulnerable shell-column region. This model may be extended to include material nonlinearity in the shell-column region for the seismic response studies. This model may also be used to study the dynamic response due to fluctuating components of wind velocity.

INTRODUCTION

Thin shell structures are built for a variety of functions. Natural draught cooling towers are built up to 590 ft (180 meter) in height to cool water heated up in the condensers so as to avoid thermal pollution of rivers, lakes, and sea shores. Chimneys are vital to power plant operation. The portion of the chimney containing flue openings behaves like a shell and is analyzed using shell theory. Storage tanks and pressure vessels are usually supported by slender columns and cylindrical skirts to provide elevation. Domes, hangars, and hypars are built on columns and walls for aesthetic and practical purposes.

Due to the slenderness of the supporting columns and the height and large dimensions of the shells, such structures are vulnerable to earthquake and wind disturbances. Evidences of failure of shell structures have not been uncommon. As recently as July 9, 1980, a shell hangar in Waterloo, Iowa, collapsed due to a wind storm. The catastrophic failure of the cooling towers at Ferrybridge, England in 1965 during a gust storm (1) and the collapse of another cooling tower at Ardeer, Scotland in 1973 (2) are the evidences of the vulnerability of the cooling towers.

Many investigators have conducted studies to better understand the stability and dynamic response behaviors of the cooling towers. Constructions of these monumental structures in the zones of high seismic risk or high wind have further intensified these investigations. In order to study the dynamic response and to properly interpret the characteristics of the loads in terms of their effect on the dynamic response of cooling towers, accurate determination of the free vibration frequencies and modes is necessary.

Early free vibration analyses for cooling towers were conducted for the cases of fixed bases. Carter, Robinson and Schnobrich (3) used numerical integration method, Hashish and Abu-Sitta (4) used a modified finite difference method, and Sen and Gould (5) developed a rotational shell finite element for such studies. A review of free vibration analysis of cooling towers can be found in Ref. 6. The presence of discrete column supports, however, significantly alters the condition of the physical restraint at the base and thereby greatly influences the dynamic response. This makes an accurate modeling of the column supports highly imperative.

A number of efforts was made to model the base column supports. Gould, Sen, and Suryoutomo (7) used a rotational shell element which possesses averaged-out properties of the individual columns. Basu and Gould (8) modified this approach and improved the results by developing a series of open type axisymmetric shell elements to model the columns. Gran and Yang (9, 10) used an alternative approach by using quadrilateral flat plate finite elements to model the shell and discrete column elements to model the columns. The advantage is that the columns were modeled more accurately but the shell is obviously modeled less efficiently as compared to that by using rotational shell elements (7,8). There appears to be a need for the development of more accurate and efficient quadrilateral shell elements by including proper curvatures. The modeling using quadrilateral shell elements and discrete column elements has the advantage and capability of obtaining detail response results, for both linear and materially nonlinear cases, in the vulnerable region of shell-column joints.

In this study, a sophisticated 3-D column element is used to model the discrete supporting columns. The response behavior of the cooling

tower shell due to earthquake load is, in general, predominantly membrane except in the vicinity of the base where bending behavior is also significant. A highly efficient high-order quadrilateral membrane element was developed by Gran and Yang (11) to be used in modeling the portion of the shell dominated by membrane forces. This element is used in combination with a quadrilateral doubly-curved general shell element (12) to model the cooling tower shell. An element formulative procedure, which is slightly different from that used in Ref. 12, is given here. An extension of this element to the analysis of buckling and vibration of a cooling tower shell under the effect of initial forces is also given. Thus an efficient modeling can be achieved by using the membrane elements and the general shell elements to model the regions dominated by membrane forces alone and by combined bending and membrane forces, respectively.

Such efficient mixed modeling requires the use of a quadrilateral transition element which is compatible with the general shell elements at the lower edge and with the pure membrane elements at the upper edge. This element is developed here.

The number of quadrilateral general shell elements needed to model the base layer of the shell has to be the same as the number of the upper joints of the supporting columns. This number can be quite high. On the other hand, the number of membrane elements needed to model an upper layer of the shell can be relatively less. A triangular membrane filler element which can connect two nodal points at the base and one on the top, and vice versa, is thus developed to fill between a fine layer and a coarse layer of quadrilateral elements.

A schematic diagram showing the modeling of a cooling tower using the five types of elements is given in Fig. 1. The five types are:

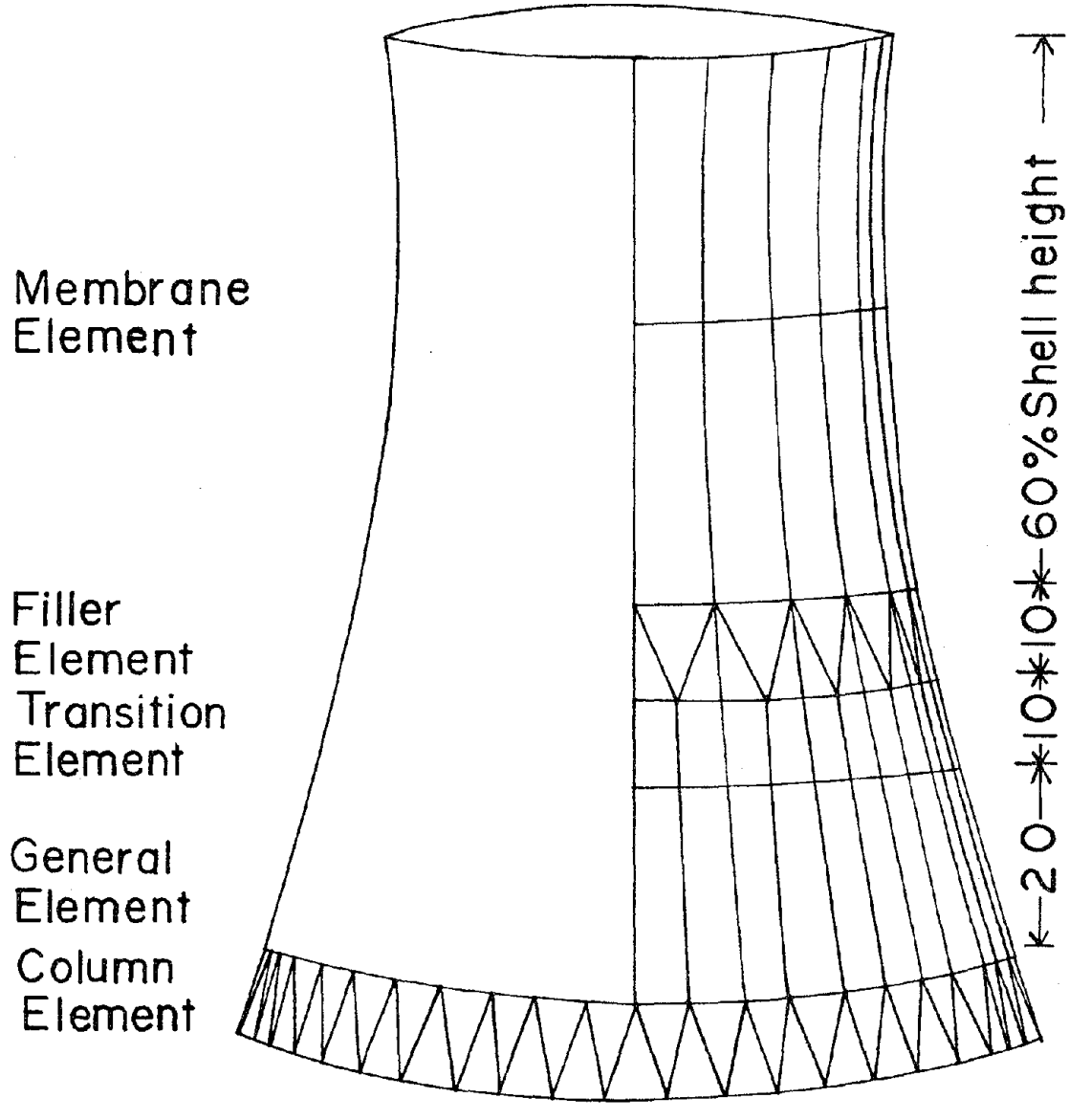

Figure 1 An Efficient Modeling for a Column-Supported Cooling Tower Using a Set of Elements.

(1) column element; (2) doubly-curved quadrilateral general shell element; (3) doubly-curved quadrilateral general-membrane transition element; (4) doubly-curved triangular filler membrane element; and (5) doubly-curved quadrilateral membrane element.

All these elements are described in greater details along with their formulative procedures in Chapter 1. A series of examples is chosen to step-by-step evaluate the performance of the elements adopted, modified and extended in this study. In Chapter 2, the whole set of elements is employed in the free vibration analysis of a column supported cooling tower. In Chapter 3, the stresses and displacements in a fixed base cooling tower due to the static component of the wind load are determined. Concluding remarks are made in Chapter 4. A brief description of the research, presently in progress, is also given in this Chapter.

CHAPTER 1

DESCRIPTION OF VARIOUS FINITE ELEMENTS AND THEIR FORMULATIONS

THE COLUMN ELEMENT

Since the supporting columns are very critical components of the cooling tower and their behavior is dominated by axial forces and axial motions, it is desirable to use a sophisticated column element that contains axial displacements as well as axial strains as degrees of freedom. A four d.o.f. bar element having both the axial displacement and the axial strain d.o.f.'s at each end was developed by Yang and Sun (13) which was proven to be highly accurate and highly efficient for axial vibration analysis. Such an element was extended in this study to the general 3-D form.

The present column element contains 8 d.o.f.'s at each of the two joints: three orthogonal displacements, u, v, and w in the η, ξ and ζ directions, respectively; two strain components $\partial u/\partial \eta$ and $\partial v/\partial \xi$; two rotations $\partial w/\partial \xi$ and $\partial w/\partial \eta$; and a rotation $\partial v/\partial \eta$ about the ζ axis. The curvilinear coordinates η, ξ and ζ are along the meridional, circumferential, and normal-to-surface directions, respectively, of the shell.

THE DOUBLY CURVED QUADRILATERAL SHELL ELEMENT

A comprehensive review of the developments of thin shell finite elements is given by Ashwell and Gallagher (14). Most notable of the developments of quadrilateral shell elements are: the 24 d.o.f. doubly-curved quadrilateral element with two constant principal radii of curvature

without rigid body modes by Gallagher (15) and a cylindrical version of the same element with rigid body modes by Cantin and Clough (16); the 48 d.o.f. cylindrical element by Bogner, Fox and Schmit (17); the 48 d.o.f. doubly-curved quadrilateral element by Greene *et al.* (18); the 48 d.o.f. quadrilateral element with two principal and a twist constant radii of curvature by Yang (19); the 48 d.o.f. quadrilateral shell of revolution element by Fonder (12); and the 28 d.o.f. quadrilateral membrane shell of revolution element by Gran and Yang (11).

The present doubly-curved quadrilateral shell element differs from Yang's element (19) in that the two opposite edges are parallel circles and the other two are along two meridional lines. The present element is essentially the same as Fonder's element (12), but this element has now been applied to perform free vibration analysis of a spherical cap, free vibration analysis of a fixed base cooling tower under the effect of initial stresses, and has also been used in combination with the other four types of elements in free vibration analysis of column supported cooling tower.

(a) Element Geometry

Fig. 2 shows a doubly-curved quadrilateral shell element and a doubly-curved triangular membrane filler element. The former is described in this section. The element is a quadrilateral defined by lines of principal curvature; thus it is rectangular in the local curvilinear coordinate system. The equations are specialized to general shells whose reference surfaces are a portion of an axisymmetric surface. An array of eight mapping nodes specifies a cubic variation of R and Z in the meridional direction. This allows an initial element geometry to exactly model meridional shapes that are third order or less. The interpolation

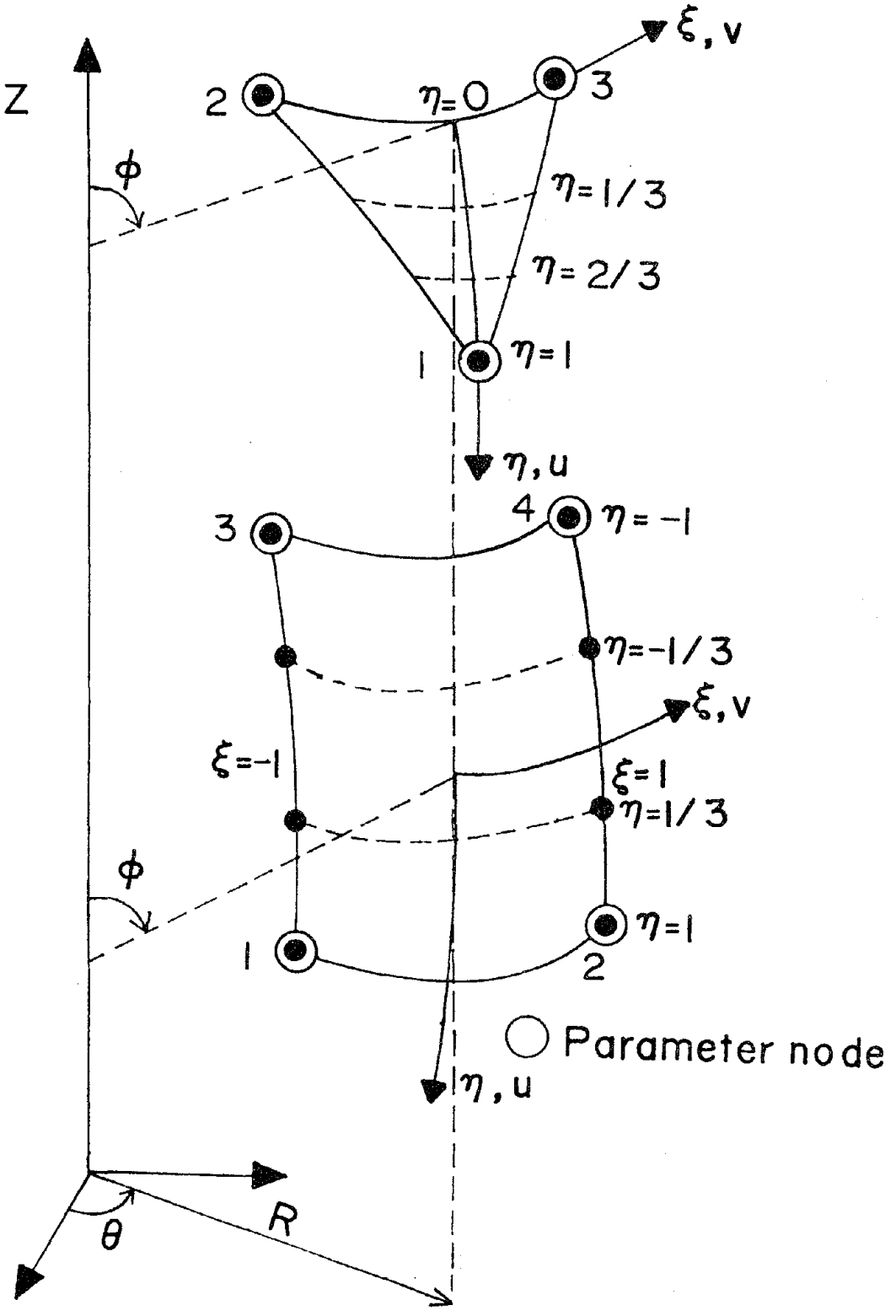

Figure 2 A Doubly-Curved Quadrilateral General Shell Element and a Doubly-Curved Triangular Membrane Filler Element.

functions for R and Z are similar so only that for R will be shown. Thus

$$R(\xi,\eta) = \sum_{i=1}^{4} M_i(\xi,\eta)R_i + \sum_{i=5}^{8} N_i(\xi,\eta)R_i \tag{1}$$

where

$$\begin{aligned} M_i(\xi,\eta) &= (1+\xi_i\xi)\ (1+\eta_i\eta)\ (9\eta^2-1)/32 \\ N_i(\xi,\eta) &= 9(1+\xi_i\xi)\ (1+9\eta_i\eta)\ (1-\eta^2)/32 \end{aligned} \tag{2}$$

The geometric parameters for the radius of curvature in meridional direction R_ϕ, and the first and second derivatives of the radius of curvature in the circumferential direction R with respect to Z are given in Ref. 11.

Other geometric relations needed in this formulation but not given in Ref. 11 are,

$$R''' = \frac{d^3R}{dZ^3} = \frac{(d^3R/d\eta^3)}{(dZ/d\eta)^3} - \left\{\frac{3(d^2R/d\eta^2)(d^2Z/d\eta^2) + (d^3Z/d\eta^3)(dR/d\eta)}{(dZ/d\eta)^4}\right\} + 3\left\{\frac{(dR/d\eta)(d^2Z/d\eta^2)^2}{(dZ/d\eta)^5}\right\} \tag{3}$$

$$\frac{\partial^2\phi}{\partial\eta^2} = (R_\phi \cos\phi)^{-1}\left\{\frac{\partial^2R}{\partial\eta^2} - \frac{\partial R}{\partial\eta}\left\{\frac{1}{R_\phi}\frac{\partial R_\phi}{\partial\eta} - \tan\phi\,\frac{\partial\phi}{\partial\eta}\right\}\right\} \tag{4}$$

where

$$\frac{\partial\phi}{\partial\eta} = \frac{(\partial R/\partial\eta)}{(\partial R/\partial\phi)} = \frac{(\partial R/\partial\eta)}{R_\phi \cos\phi} \tag{5}$$

and the value of $\partial R_\phi/\partial\eta$ is determined as

$$\frac{\partial R_\phi}{\partial\eta} = -\left\{3R'\,[1+(R')^2] - \frac{[1+(R')^2]^{\frac{3}{2}}\,R'''}{(R'')^2}\right\}\frac{dZ}{d\eta} \tag{6}$$

Variation of θ in the circumferential direction is implicitly assumed to be linear. Hence

$$\frac{\partial\theta}{\partial\xi} = \frac{\Delta\theta}{2} \tag{7}$$

where $\Delta\theta$ is the angle subtended by the shell element in the circumferential direction.

To illustrate the preceding discussion, a spherical cap shown in a later figure, will be examined. The cap subtends an angle of 5°-44' in the meridional direction. If a portion of the shell, say $\Delta\theta = 5°$, is modeled using one finite element, the following relations will be calculated at the central Gauss point: $\partial R/\partial\eta = 4.9937$, $\partial\phi/\partial\eta = 0.050$, and $\partial\theta/\partial\xi = 0.0436$. In this case the derivatives $\partial\phi/\partial\eta$ and $\partial\theta/\partial\xi$ will be constant over the element surface.

(b) Displacement Functions

The element possesses 12 d.o.f.'s at each of the four vertices: u; $\partial u/\partial\xi$; $\partial u/\partial\eta$; $\partial^2 u/\partial\xi\partial\eta$; v; $\partial v/\partial\xi$; $\partial v/\partial\eta$; $\partial^2 v/\partial\xi\partial\eta$; w; $\partial w/\partial\xi$; $\partial w/\partial\eta$; $\partial^2 w/\partial\xi\partial\eta$. The displacement functions for u, v, and w are assumed to be of the same form, each consisting of a bicubic Hermite polynomial in ξ and η. Development and justification of such assumed displacement functions were given in Refs. 17, 18, 19 and 12.

(c) Element Formulation

The strain-displacement relations used in this study are based on those from Love's theory and are given in Ref. 20 in the general form. The equations are specialized for shallow shells of revolution by putting $A_1 = R_\phi$ and $A_2 = R$. A_1 and A_2 are the Lame's parameters. Furthermore, the shell is assumed to be thin such that h/R and h/R_ϕ are negligible as

compared to unity, h being the thickness of the shell. The following strain-displacement relations are used in the present study.

$$\varepsilon_\phi = \frac{1}{R_\phi}\frac{\partial u}{\partial \phi} + \frac{w}{R_\phi}$$

$$\varepsilon_\theta = \frac{\cos\phi}{R} u + \frac{1}{R}\frac{\partial v}{\partial \theta} + \frac{\sin\phi}{R} w \tag{8}$$

$$\varepsilon_{\phi\theta} = \frac{1}{R}\frac{\partial u}{\partial \theta} + \left(\frac{1}{R_\phi}\frac{\partial}{\partial \phi} - \frac{\cos\phi}{R}\right) v$$

$$\kappa_\phi = -\frac{1}{R_\phi^2}\frac{\partial^2 w}{\partial \phi^2} - \left(u - \frac{\partial w}{\partial \phi}\right)\frac{1}{R_\phi^3}\frac{\partial R_\phi}{\partial \phi}$$

$$\kappa_\theta = -\frac{1}{R^2}\frac{\partial^2 w}{\partial \theta^2} \tag{9}$$

$$\kappa_{\phi\theta} = -2\left(\frac{1}{RR_\phi}\frac{\partial^2 w}{\partial \phi \partial \theta} - \frac{\cos\phi}{R^2}\frac{\partial w}{\partial \theta}\right)$$

Eqs. 8 and 9 correspond to the mid-surface strains and the curvatures respectively. The validity of the above strain-displacement relations will be substantiated by the results presented subsequently. Various derivatives required in the above expressions are in terms of global coordinates. These can be determined by differentiating the shape functions in local coordinates and then employing the coordinate transformation as given below.

$$\begin{Bmatrix} \partial N/\partial \theta \\ \partial N/\partial \phi \end{Bmatrix} = [J]^{-1} \begin{Bmatrix} \partial N/\partial \xi \\ \partial N/\partial \eta \end{Bmatrix} \tag{10}$$

where the Jacobian matrix is given as

$$[J] = \begin{bmatrix} \partial\theta/\partial\xi & 0 \\ 0 & \partial\phi/\partial\eta \end{bmatrix} \tag{11}$$

The second derivatives with respect to θ and ϕ are obtained as

$$\frac{\partial^2 N}{\partial \theta^2} = \left(\frac{\partial \theta}{\partial \xi}\right)^{-2} \left(\frac{\partial^2 N}{\partial \xi^2}\right) \tag{12}$$

$$\frac{\partial^2 N}{\partial \phi^2} = \left(\frac{\partial \phi}{\partial \eta}\right)^{-2} \left(\frac{\partial^2 N}{\partial \eta^2}\right) - \left(\frac{\partial \phi}{\partial \eta}\right)^{-3} \left(\frac{\partial N}{\partial \eta}\right) \left(\frac{\partial^2 \phi}{\partial \eta^2}\right) \tag{13}$$

and

$$\frac{\partial^2 N}{\partial \phi \partial \theta} = \left[\left(\frac{\partial \phi}{\partial \eta}\right)\left(\frac{\partial \theta}{\partial \xi}\right)\right]^{-1} \frac{\partial^2 N}{\partial \xi \partial \eta} \tag{14}$$

Element stiffness matrix [k] is then obtained by performing the following volume integration

$$[k] = \int_V [B]^T [D][B] dV \tag{15}$$

where [B] is a 6x48 matrix which relates the 6 components of the strain vector to the 48 components of the elemental d.o.f.'s and D is a 6x6 stress-strain matrix.

The differential volume dV is defined as

$$dV = hdA = hR_\phi \, d\phi \; R \, d\theta \; = hRR_\phi |J| \, d\xi d\eta \tag{16}$$

The element stiffness matrix can now be determined using a 5 by 5 Gaussian quadrature as

$$[k] = \sum_{i=1}^{5} \sum_{j=1}^{5} [B]^T [D][B] \, W_i W_j hRR_\phi |J| \tag{17}$$

where W_i and W_j are the Gauss weight factors at the 5x5 Gauss points.

The consistent mass matrix [m] and the incremental stiffness matrix [n] are obtained as

$$[m] = \sum_{i=1}^{5} \sum_{j=1}^{5} [N]^T [N] \rho W_i W_j \; hRR_\phi |J| \tag{18}$$

$$[n] = \sum_{i=1}^{5} \sum_{j=1}^{5} [G]^T \begin{bmatrix} N_\phi & N_{\phi\theta} \\ N_{\theta\phi} & N_\theta \end{bmatrix} [G] W_i W_j R R_\phi |J| \qquad (19)$$

where N_ϕ, N_θ, and $N_{\phi\theta}$ are the components of middle-surface stress resultants. These stress resultants (also known as the "initial stresses") can be obtained by using a simple pre-buckling membrane analysis or a more rigorous iterative analysis as described by Gallagher and Yang (21). Matrix [G] relates the two rotations and the 48 d.o.f.'s as

$$\begin{Bmatrix} \beta_\phi \\ \beta_\theta \end{Bmatrix} = [G]\{q\} \qquad (20)$$

The two rotations are defined as

$$\begin{Bmatrix} \beta_\phi \\ \beta_\theta \end{Bmatrix} = \begin{bmatrix} 1/R_\phi & 0 & -(\partial/\partial\phi)/R_\phi \\ 0 & \sin\phi/R & -(\partial/\partial\theta)/R \end{bmatrix} \begin{Bmatrix} u \\ v \\ w \end{Bmatrix} \qquad (21)$$

It is felt that the compatibility of each of the three d.o.f.'s ($\partial^2 u/\partial\xi\partial\eta$; $\partial^2 v/\partial\xi\partial\eta$; and $\partial^2 w/\partial\xi\partial\eta$) at each of the four vertices of an element with that of the adjacent elements may be relaxed by writing them in terms of the rest of the 36 d.o.f.'s at the element level before assemblage. This can be done by matrix partitioning and substitution with the assumption that the counterpart forces corresponding to these cross derivative d.o.f.'s are zero.

The element stiffness, mass and incremental stiffness matrices thus obtained are in terms of local coordinates ξ and η. Transformation of these three matrices as well as the nodal forces and the d.o.f.'s to those with reference to global coordinates is performed before assemblage.

Element load, stiffness, mass and incremental stiffness matrices are then assembled in the usual manner to form the corresponding global matrices in the following set of equations of motion.

$$[M]\{\ddot{q}\} + [K]\{q\} + [N]\{q\} = \{P\} \tag{22}$$

These equations reduce to

$[K]\{q\} = \{P\}$ for static analysis;

$[K]\{q\} - [N]\{q\} = 0$ for stability analysis;

$[M]\{\ddot{q}\} + [K]\{q\} = 0$ for free vibrations analysis; and

$[M]\{\ddot{q}\} + [K+N]\{q\} = 0$ for free vibrations analysis under the effect of initial stresses.

(d) Evaluative Analysis

Before applying this element along with the other four types of elements to analyze the cooling towers, its performance to the shell problems of static load, free vibration, buckling and free vibration under the initial membrane stresses was evaluated.

(i) Rigid Body Modes - Finite element displacement functions must be so chosen that mesh refinement results in monotonic and rapid convergence of the solution.

An investigation on how well the rigid-body modes are included in the displacement functions can be made by performing the eigenvalue analysis of the element stiffness matrix.

$$[[k] - \lambda[I]]\{q\} = 0 \tag{23}$$

In the present study, the eigenvalue analysis of the stiffness matrix was performed based on two sets of assumed parameters. The results are given in Table 1. In each set of results, the presence of six rigid-body modes

TABLE 1. -- Eigenvalues of the 36 d.o.f. General Shell Element

Case 1 (1)	Case 2 (2)
-1.288×10^{-8}	8.486×10^{-9}
-5.600×10^{-9}	1.716×10^{-7}
1.513×10^{-5}	3.594×10^{-7}
2.919×10^{-5}	2.921×10^{-4}
2.923×10^{-5}	2.934×10^{-4}
9.629×10^{-5}	1.244×10^{-3}
7.056×10^{1}	1.948×10^{1}
5.211×10^{2}	6.094×10^{2}
6.381×10^{2}	7.251×10^{2}
6.931×10^{2}	8.125×10^{2}
.	.
.	.
.	.
3.244×10^{6}	1.15×10^{7}

Spherical Element: Young's modulus = 10^7 psi; (69.75 GN/m); Poisson's ratio = 0.3; thickness = 0.1 in. (2.54 mm); radii of curvature = 100 in. (2.54 m); element length = width = 8 in. (20.32 cm) for Case 1 and 16 in. (40.64 cm) for Case 2.

is clearly demonstrated by the six near zero eigenvalues.

(ii) A Fixed-Base Cooling Tower Under its Own Weight -- This problem is axisymmetric and predominated by membrane behavior. When quadrilateral elements are used, only a strip of the shell need be analyzed. The geometric parameters were defined as: radius at the base = 127.2 ft. (38.77 m); radius at the throat = 70.29 ft. (21.42 m); radius at the top = 73.10 ft. (22.28 m); height = 331.81 ft. (101.14 m); and the height from the throat to top = 80.24 ft. (24.46 m); thickness = 0.5 ft. (15.24 cm). Modulus of elasticity = 4.32×10^8 lbs/ft^2 (20.92 GN/m^2); the weight density = 150 lbs/ft^3 (23.837 KN/m^3); and Poisson's ratio = 0.2.

This problem was analyzed by Larsen (22) using refined axisymmetric elements and by Fonder and Clough (23) using 20 24-d.o.f. doubly-curved quadrilateral shell elements (122 d.o.f.'s) to model a strip. Both analyses gave almost identical results in membrane forces which are shown in Fig. 3. Due to the negative Gaussian curvature, the explicit inclusion of rigid-body modes, in Ref. 23, yielded erroneous results and thus they were excluded in obtaining the correct solution.

Gran and Yang (11) used the quadrilateral high-order membrane elements to analyze this problem and the elements were proven to be highly accurate and efficient. Their meridional membrane forces were in slight error at the base of the shell because their elements lacked the capability of modeling the bending behavior.

In this analysis, a strip of the shell with a subtending angle of 5° was analyzed. Three meshes were used: 3x1 mesh (28 d.o.f.'s): 5x1 mesh (44 d.o.f.'s) and 7x1 mesh (60 d.o.f.'s). The results are also shown in Fig. 3. It is seen that excellent results were obtained at the 3 element level.

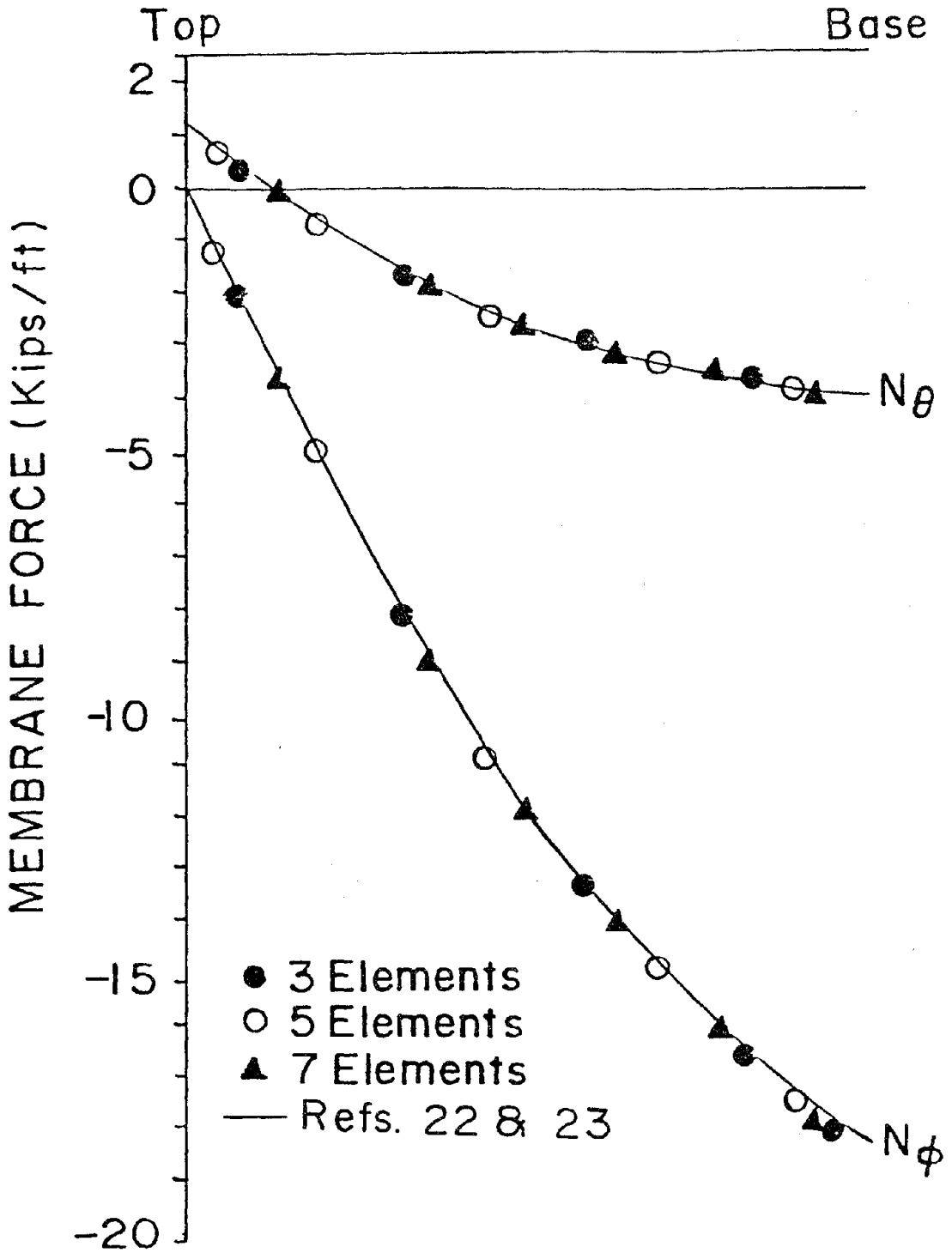

Figure 3 Circumferential Force (N_ϕ) and Meridional Force (N_θ) in a Cooling Tower Under its Own Weight (1 lb = 4.45 N, 1 ft = 0.305 m).

The relaxation of the inter-nodal compatibility of the d.o.f.'s containing the second order cross derivatives of the displacements was also investigated. Because the cross-derivative d.o.f.'s were eliminated at the element level, the boundary conditions that $\partial^2 u/\partial\phi\partial\theta = \partial^2 v/\partial\phi\partial\theta = \partial^2 w/\partial\phi\partial\theta = 0$ could not be met. Although the results were acceptable, the effect due to relaxation of such compatibility could not be determined with such an example.

(iii) Orthotropic Cylindrical Shell Under Internal Pressure -- This problem is described in Fig. 4. Four elements were used to model an octant and the results for bending moment along the axial direction and the circumferential stress resultants are plotted in Fig. 4. The analytical solutions by Kraus (24) are also shown. Excellent agreement is seen.

(iv) Axisymmetric Vibration of a Clamped Spherical Cap -- The problem was analyzed by Kalnins (25) who derived the frequency equations in terms of Legendre's polynomials with complex indices. It was also solved numerically by Zarghamee and Robinson (26) using Holzer's method. In that method, a value of the natural frequency is repeatedly assumed and the governing two point boundary value problem is solved as a set of initial value problems until all the boundary conditions are satisfied.

In this study, a sector with a subtending angle of 5° was analyzed. Natural frequency for the lowest axisymmetric mode was obtained by using both consistent and lumped mass matrices for gradually increasing number of elements. The results are shown in Fig. 5. The frequency obtained by using consistent mass matrix converged to that of Ref. 26 at the 3 element level (22 d.o.f.'s) and the frequency obtained by using lumped mass matrix is converging at a rather slow rate.

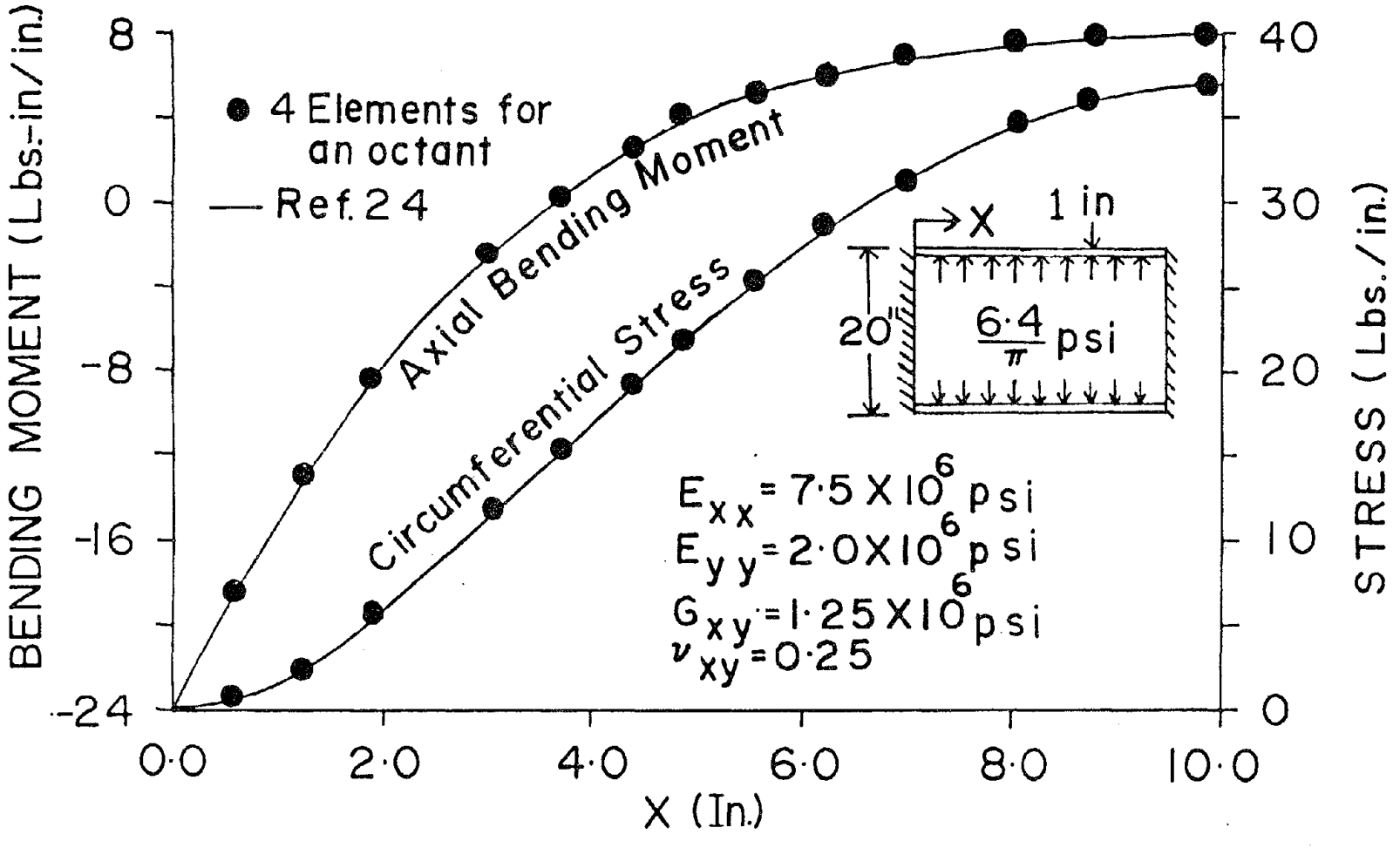

Figure 4 Axial Bending Moment and Circumferential Stress Resultant Along the Length of the Orthotropic Cylinder (Length = 20 in; 1 in. = 2.54 cm, lb. = 4.45 N)

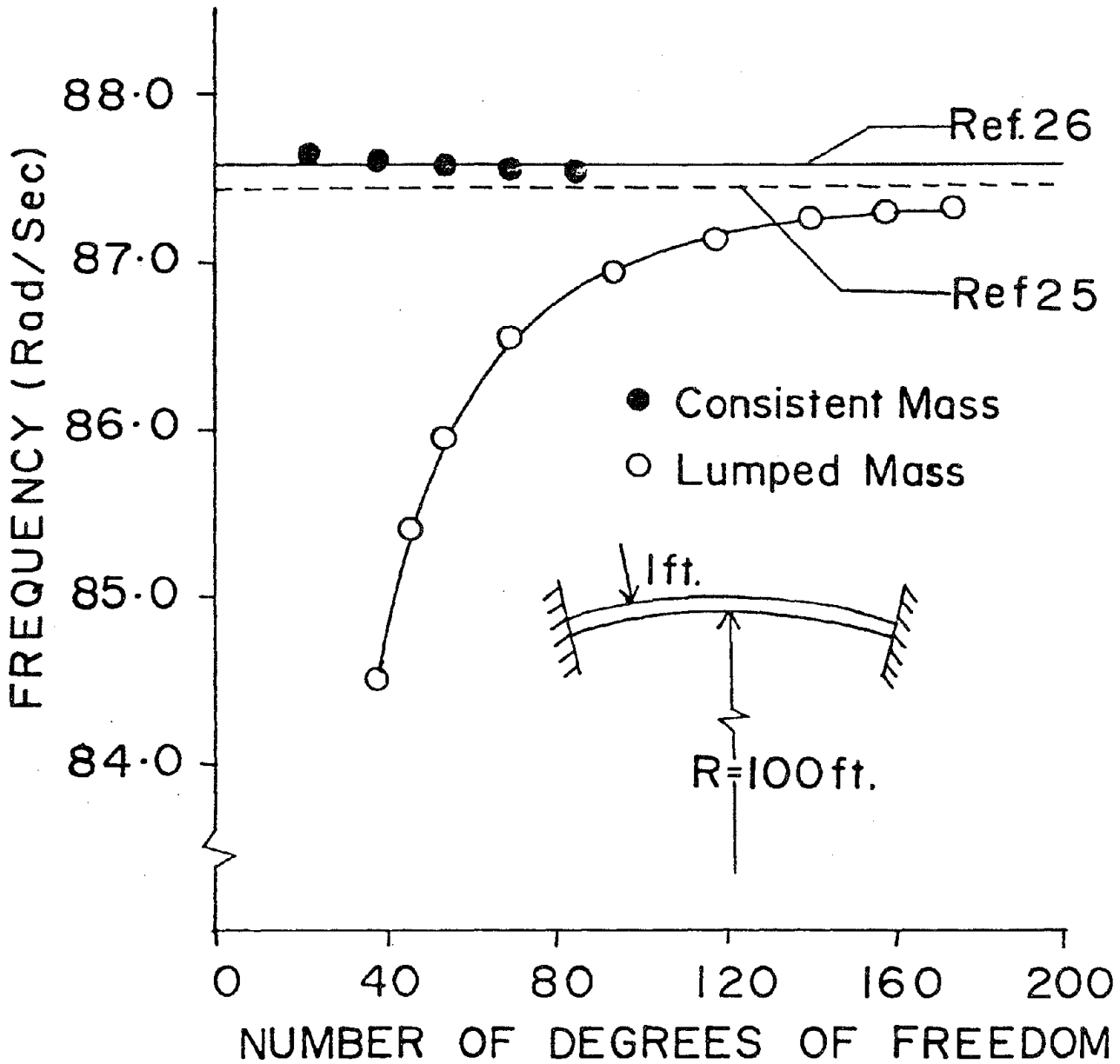

Figure 5 Axisymmetric Vibration of a Spherical Cap with Subtending Angle of 11.28°, $E = 3 \times 10^7$ psf, $\nu = 0.3$ and $\rho = 4.5$ lb. sec^2/ft^4 (1 lb = 4.45 N, 1 ft = 0.305 m).

(v) Axisymmetric Buckling of a Simply-Supported Cylindrical Shell Under Uniform Axial Compressive Stress -- This example was chosen to verify the accuracy of the incremental stiffness matrix. Only an octant of the shell was modeled using one element in the circumferential direction and different numbers of elements in the axial direction. The simply supported boundary conditions were assumed such that all the initial stress resultants other than that in the axial direction were zero. The buckling stress was found to be 0.6077 Eh/a as compared to the classical value of 0.6052 Eh/a (27), where E is the Modulus of Elasticity, h is thickness and a is the mean radius of the cylinder. The analysis was carried out using h = 1 in. and Eh/a = 1. The value obtained was found to be about 0.4% higher than the classical value.

(vi) Free Vibrations of a Fixed Base Cooling Tower Without and With Initial Stresses -- The geometry of the cooling tower is defined as: radius at the base = 137 ft. (41.76 m); radius at the throat = 84 ft. (25.6 m); radius at the top = 87.4 ft. (26.64 m); height of the tower = 330 ft. (100.59 m); height between the top and the throat = 60 ft. (18.29 m); and the thickness = 5 in. (12.7 cm). Material properties are: Modulus of Elasticity = $3x10^6$ psi (20.92 GN/m^2); Poisson's ratio = 0.15; and mass density = 0.000225 $lbs\text{-}sec^2/in^4$ (2406.5 kg/m^3).

The natural frequencies for various modes for this example were obtained by using various methods (3,4,5). These results are given in Table 2. A convergence study was first performed by using the 36 d.o.f. elements (without the cross derivative d.o.f.'s) to model a half of the cooling tower to obtain the natural frequencies for the first eccentric mode (m=n=1). The values of these frequencies were found to be 3.400, 3.320, and 3.317 Hz. when the 4x1 (50 d.o.f.'s), 4x2 (87 d.o.f.'s), and

5x3 mesh (146 d.o.f.'s) were used, respectively, where MxN mesh is defined as M elements in the meridional direction and N elements in the circumferential direction, respectively. The values of natural frequencies for this mode obtained in Refs. 3, 4 and 5 were 3.290, 3.335, and 3.291 Hz., respectively.

The natural frequencies for various modes were then studied by using the 5x3 mesh to model two different kinds of strips: (1) a strip containing half of circumferential wave, i.e., from peak to valley of a full wave and (2) a strip containing a quarter of a circumferential wave. For strip 1, the two meridional edges have the same conditions: $v = \partial u/\partial \xi = \partial^2 u/\partial \xi \partial \eta = \partial v/\partial \eta = \partial w/\partial \xi = \partial^2 w/\partial \xi \partial \eta = 0$. For strip 2, one meridional edge has the same conditions as those for strip 1 but the other edge has the conditions that $u = \partial u/\partial \eta = w = \partial w/\partial \eta = \partial v/\partial \xi = \partial^2 v/\partial \xi \partial \eta = 0$. Although both the 48 and 36 d.o.f. elements were used, the 36 d.o.f. elements could not satisfy the edge conditions when the aforementioned second order cross derivatives of displacements vanish. The results are given in Table 2. It is seen that all fhe results are generally in good agreement with those obtained in Refs. 3, 4 and 5. The results given in column 9 using the 48 d.o.f. elements for modeling 2 appear to be the most accurate ones and such model was used in the subsequent free vibration analysis when the initial stresses were considered.

Three types of initial stresses were then considered: uniform circumferential compressive stress; uniform meridional compressive stress; and membrane stresses due to self weight of the cooling tower.

The effects of uniform circumferential and meridional stresses on the square of the frequency ratio $(\omega/\omega_0)^2$ for several modes are shown in Figs. 6 and 7, respectively, where ω_0 is the frequency value with no

TABLE 2 -- Natural Frequencies of a Fixed Base Cooling Tower for Various Modes (n = circumferential Wave number and m = Longitudinal Mode Number).

n (1)	m (2)	NATURAL FREQUENCY IN HERTZS							
					36 d.o.f. element		48 d.o.f. element		
								Modeling 2†	
		Carter et al. Ref. (3) (3)	Hashish and AbuSitta Ref. (4) (4)	Sen and Gould Ref. (5) (5)	Modeling 1* (6)	Modeling 2† (7)	Modeling 1* (8)	Without Self-Weight (9)	With Self-Weight (10)
1	1	3.2897	3.3345	3.2910	3.3166	3.3137	3.2897	3.2901	3.2898
	2	6.7932	6.8816	6.8176	7.1098	7.0656	6.7935	6.7958	6.7950
	3	10.525	10.532	10.667	11.664	--	10.604	10.624	10.616
2	1	1.7661	1.7848	1.7662	1.7744	1.7723	1.7684	1.7683	1.7666
	2	3.6946	3.7234	3.6960	3.7607	3.7510	3.6919	3.6953	3.2926
	3	6.9590	6.9553	7.0058	7.5649	7.4466	6.9607	6.9813	6.9769
3	1	1.3755	1.3927		1.3802	1.3731	1.3821	1.3809	1.3732
	2	1.9912	2.0150		2.0228	1.9982	1.9986	1.9996	1.9927
	3	4.3272	4.3353		4.4863	4.4536	4.3483	4.3595	4.3522
4	1	1.1812	1.2003	1.1820	1.1677	1.1512	1.1906	1.1885	1.1653
	2	1.4481	1.4597	1.4491	1.4367	1.4195	1.4629	1.4615	1.4498
	3	2.7788	2.7762	2.7866	2.8072	2.7946	2.7902	2.7941	2.7814
5	1	1.0352	1.0441	1.0354	--	--	1.0522	1.0489	1.0131
	2	1.4299	1.4417	1.4345	1.3834	1.3455	1.4509	1.4489	1.4181
	3	2.0568	2.0558	2.0640	2.0365	2.0149	2.0721	2.0714	2.0558
6	1	1.1472	1.1544				1.1700	1.1667	1.1084
	2	1.3236	1.3335				1.3530	1.3560	1.3138
	3	2.0149	2.0152				2.0345	2.0364	2.0104
7	1	1.3020	1.3055				1.3253	1.3224	1.2458
	2	1.5140	1.5189				1.5482	1.5450	1.4943
	3	1.9225	1.9200				1.9572	1.9553	1.9162

*Modeling of a strip containing half of a circumferential wave.

†Modeling of a strip containing quarter of circumferential wave.

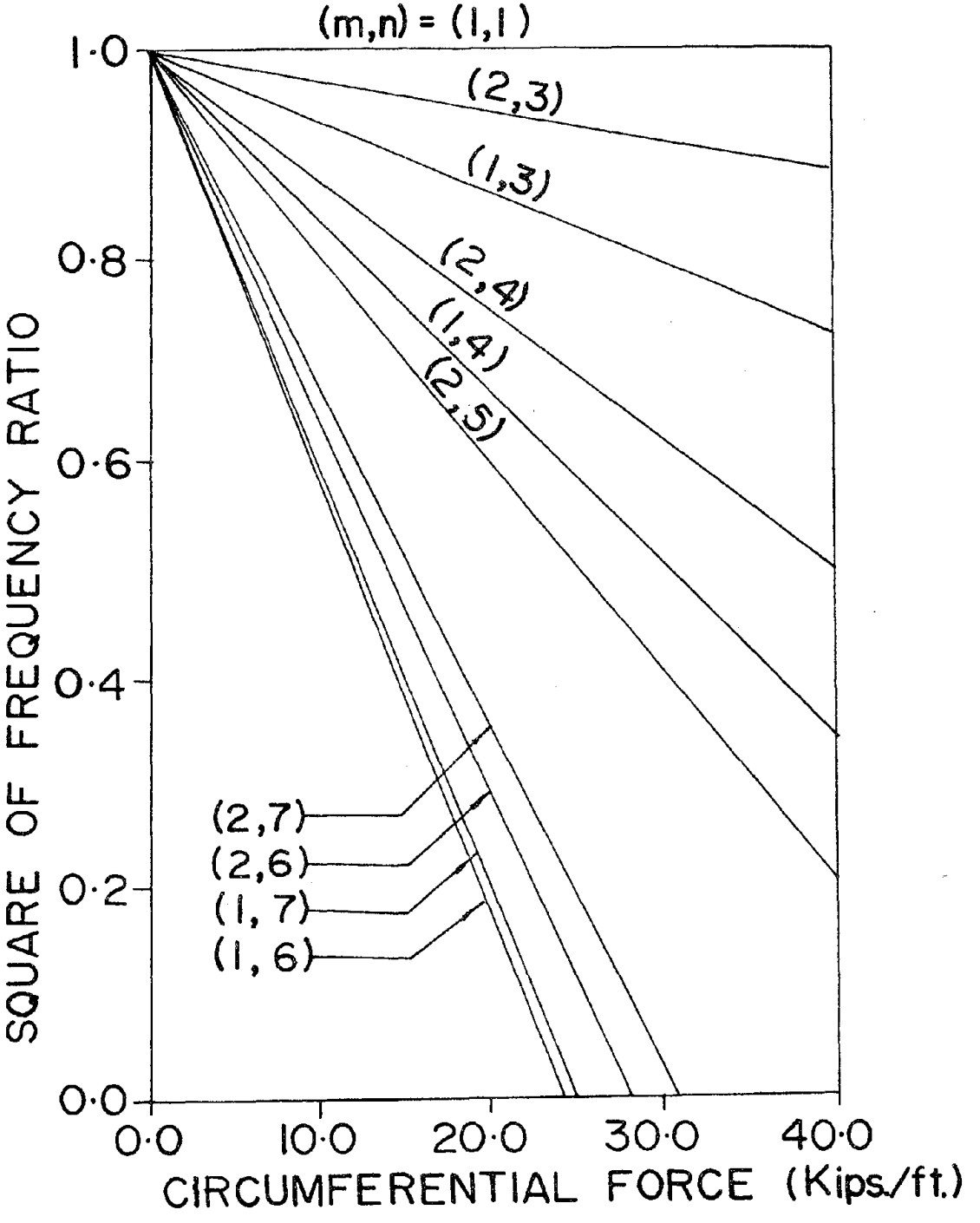

Figure 6 Effect of Uniform Circumferential Force on Frequency Ratio for a Fixed Base Cooling Tower for Various Modes (m = Number of Meridional Mode; n = Number of Circumferential Waves; 1 lb = 4.45 N, 1 ft. = 0.305 m).

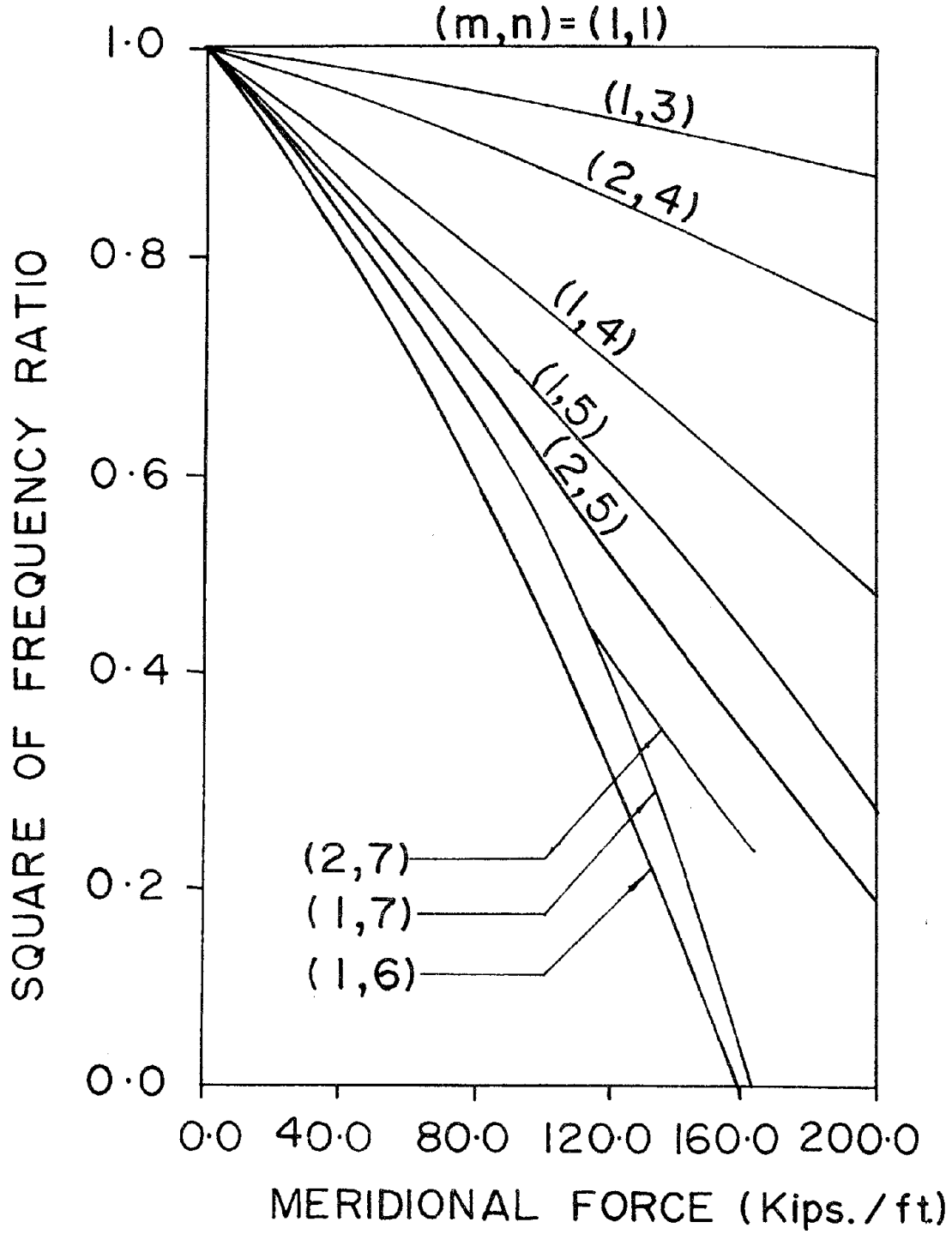

Figure 7 Effect of Uniform Meridional Force on Frequency Ratio for a Fixed Base Cooling Tower for Various Modes (m = Number of Meridional Mode; n = Number of Circumferential Waves; 1 lb = 4.45 N, 1 ft = 0.305 m).

initial stresses. This problem was studied previously by Deb Nath (28) using revolutional type of shell elements. The present results in Figs. 6 and 7 are in total agreement with those given in Ref. 28, which are thus not replotted here.

It is seen in Fig. 6 that for each mode considered, $(\omega/\omega_0)^2$ varies linearly with the uniform circumferential stress, which is equal to its buckling value as ω becomes zero. This linear relation suggests that the mode shapes do not change as the circumferential stress increases.

In Fig. 7, however, $(\omega/\omega_0)^2$ for each mode varies nonilnearly with the uniform meridional stress, suggesting that each mode changes its shape as the meridional stress increases.

The frequency-stress relation shown in Fig. 7 for the first eccentric mode (m=n=1) appears to be a horizontal straight line. No appreciable change in the natural frequency corresponding to this mode was observed even up to a uniform compressive force of 200 kips/ft. When the mode shapes for u, v, and w displacements were plotted, they were found to be the same as those shown in Refs. 3,4,9, and 11, respectively, and remain almost independent of the level of meridional stress considered.

The frequency-stress relation for the mode (m=1, n=6) is nonlinear and decreases rapidly. The meridional mode shape for w deflection was plotted for four different values of meridional stresses in Fig. 8. The effect of meridional stress on the shape for this mode is obvious.

The effect of self weight on the natural frequencies was studied next. The membrane stresses due to the self weight were calculated at all the 25 Gaussian points for every element. The use of numerical integration allows this element to take into account the variable initial stresses. The natural frequencies obtained for the cooling tower

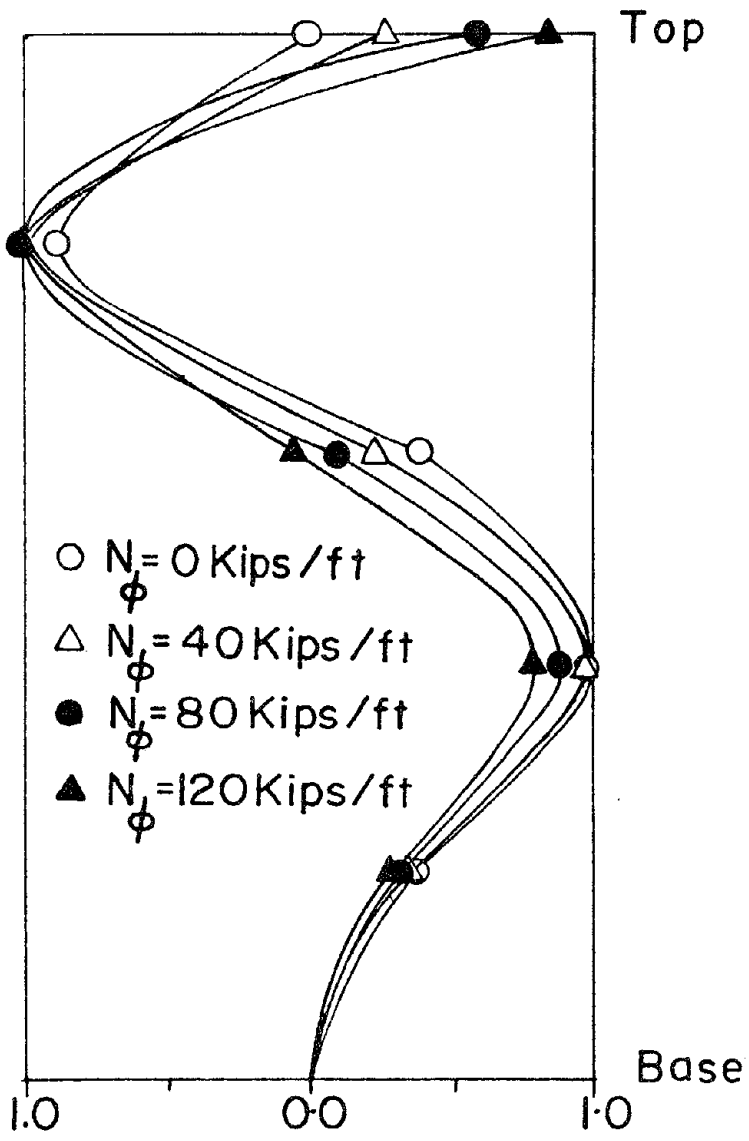

Figure 8 Effect of Uniform Meridional Stress Resultant (N_ϕ) on the Shape of the (m=1, n=6) Mode of the Fixed Base Cooling Tower.

considering its own weight are shown in column 10 of Table 2. The values were found to change very little due to self weight, at the most a few percent for higher modes.

THE QUADRILATERAL GENERAL-MEMBRANE TRANSITION ELEMENT

Previous investigations on the dynamic response of a cooling tower (9, 10) suggest that the behavior of the shell is predominantly membrane except that near the base. It appears to be efficient to use two types of elements, a membrane type and a general type, to model the upper portion and the base portion of the shell, respectively. A high-order and highly efficient quadrilateral membrane element was developed by Gran and Yang (11) and a quadrilateral general shell element developed by Fonder (12) was extended in this study. There is a need to develop a quadrilateral bending-membrane transition element so that its upper and lower edges are compatible with the membrane and general shell elements, respectively.

The geometry of this quadrilateral transition element is identical to that of the membrane (11) or the general shell element (Fig. 2). Each of the two upper corner points has the same 9 d.o.f.'s as those assumed for the membrane element: u; $\partial u/R\partial\theta$; $\partial u/R_\phi\partial\phi$; $\partial^2 u/R\partial\theta R_\phi\partial\phi$; v; $\partial v/R\partial\theta$; $\partial v/R_\phi\partial\phi$; $\partial^2 v/R\partial\theta R_\phi\partial\phi$; and w. Each of the two lower corner points has the same 12 d.o.f.'s as those assumed for the present shell element.

The membrane displacement functions u and v for this transition element are assumed to be the same as those for the membrane or the general shell elements. The function describing the normal-to-the-surface deflection is assumed as

$$w = \sum_{i=1}^{2} [G_i(\xi)G_i(\eta)w_i + H_i(\xi)G_i(\eta)\left(\frac{\partial w}{\partial \xi}\right)_i + G_i(\xi)H_i(\eta)\left(\frac{\partial w}{\partial \eta}\right)_i$$

$$+ H_i(\xi)H_i(\eta)\left(\frac{\partial^2 w}{\partial \xi \partial \eta}\right)_i] + \sum_{i=3}^{4} G_i(\xi)G_i(\eta)w_i \tag{24}$$

where $G_i = (-\xi_i\xi^3 + 3\xi_i\xi + 2)/4$ and $H_i = (\xi^3 + \xi_i\xi^2 - \xi - \xi_i)/4$ and subscript i indicates the nodal point number shown in Fig. 2.

This transition element has a total of 42 d.o.f.'s of which 10 are for the second order cross derivatives of u, v, and w, respectively. The inter-nodal point compatibility of the cross derivatives d.o.f.'s may be relaxed by writing them in terms of the rest of the 32 d.o.f.'s.

The formulation of this transition element was evaluated by using this type and the other two types of elements (the general shell elements and the membrane elements) to compare the natural frequency for first eccentric mode (m=n=1) for the fixed base cooling tower considered in the previous section. This mode is the most dominant one in the earthquake response of cooling towers (29). Two modelings were used to model half of the cooling tower: (1) 2 general shell elements at the base, 2x2 membrane elements at the top, and 2 transition elements; (2) 3 general shell elements at the base, 2x3 membrane elements at the top, and 3 transition elements. Both modelings gave the same natural frequency of 3.32 Hz. This value appears to be accurate as compared to those given in the first row of Table 2.

THE TRIANGULAR FILLER MEMBRANE ELEMENT

When the supporting columns of a cooling tower are modeled by using discrete column elements, a layer of quadrilateral general shell elements

providing the same number of joints at the base of the shell as that of the top joints of the columns is needed. For more efficient modeling of a cooling tower when its behavior is predominantly membrane, however, a coarser mesh of the quadrilateral membrane elements may be used to model the upper portion of the shell. There appears to be a need to develop a triangular filler type of elements, as shown in Fig. 1, which can connect the coarser mesh of the quadrilateral membrane elements to the finer mesh of the quadrilateral general-membrane transition elements.

A number of doubly-curved general shell elements of triangular shape are available (14). The ones that are pertinent to the present development of the triangular filler elements are mentioned here. Cowper, Lindberg, and Olson (30) developed a 36 d.o.f. triangular shallow shell element. Each vertex contained 12 d.o.f.'s: u; $\partial u/\partial \xi$; $\partial u/\partial \eta$; v; $\partial v/\partial \xi$; $\partial v/\partial \eta$; w; $\partial w/\partial \xi$, $\partial w/\partial \eta$; $\partial^2 w/\partial \xi^2$; $\partial^2 w/\partial \xi \partial \eta$; and $\partial^2 w/\partial \eta^2$, where ξ and η are the coordinates in the plane of the projection. The displacement function for u or v was assumed as a complete cubic polynomial in ξ and η (10 constants) and that for w a complete quintic polynomial minus the $\xi^4\eta$ term to ensure that $\partial w/\partial \eta$ along the edge $\eta = 0$ is in the form of a cubic polynomial in ξ (20 constants). Two extra d.o.f.'s were created at the centroid of the element. The 40 constants exceed the 38 d.o.f.'s by 2. Two further constraints were imposed to ensure that the slopes normal to the remaining two edges ($\partial w/\partial n$) are also in the form of a cubic polynomial.

Thomas and Gallagher (31) developed a 27 d.o.f. triangular shell element. Each vertex contained 9 d.o.f.'s: u, $\partial u/\partial \xi$, $\partial u/\partial \eta$; v; $\partial v/\partial \xi$; $\partial v/\partial \eta$; w; $\partial w/\partial \xi$; and $\partial w/\partial \eta$ where ξ and η are the curvilinear coordinates in the middle surface. Each of the three displacement functions u, v, and w was assumed as a complete cubic polynomial in ξ and η (10 constants).

Three d.o.f.'s of u, v and w are added at the centroid of the element so that the 30 constants can be determined by the 30 d.o.f.'s. The assumption of such a displacement field violates the conditions of interelement compatibility, in that normal rotations are not continuous across the element boundaries. This results in the global strain energy being improperly defined. This difficulty was overcome by writing constraint equations which force the normal rotations at the mid-side of each edge to be the same for adjacent elements. The constraint equations produced in this manner were accounted for in the global analysis by the use of the Lagrange multiplier technique. This is done by augmenting the potential energy with the sum of the products of the respective constraint conditions and their corresponding Lagrange multipliers.

Dawe (32) developed a 54 d.o.f. triangular shallow shell element. Each vertex contained 18 d.o.f.'s: u; $\partial u/\partial \xi$; $\partial u/\partial \eta$; $\partial^2 u/\partial \xi^2$; $\partial^2 u/\partial \xi \partial \eta$; $\partial^2 u/\partial \eta^2$; and the similar six for v and w, respectively, where ξ and η are the coordinates in the plane of the projection with ξ coinciding with one edge of the element. Each of the three displacement functions u, v, and w was assumed as a complete quintic polynomial in ξ and η minus the $\xi^4\eta$ term to ensure that the variation of each of the three slopes $\partial u/\partial \eta$, $\partial v/\partial \eta$, and $\partial w/\partial \eta$ along the edge $\xi = 0$ is in the form of a cubic polynomial (20 constants). Six further constraints were imposed to ensure that the derivatives of u, v, and w with respect to the axis normal to the other two edges are also in the form of cubic polynomials.

Two types of triangular filler membrane elements were formulated in this study. The formulation for the first type follows the developments of Refs. 30 and 31 and that for the second type follows the development of Ref. 32. Both types have the same geometry.

(a) Element Geometry

The geometry of either type of the triangular membrane element is shown in Fig. 2. The local curvilinear coordinates ξ and η lie along the circumferential and meridional directions, respectively, of the surface of a shell of revolution. The edge 2-3 lies on the ξ-axis and the η-axis passes through nodal point 1.

The cylindrical coordinates R and Z for an arbitrary point on the element surface are described as

$$R = \sum_{i=1}^{4} N_i R_i \tag{25}$$

where R_1, R_2, R_3, and R_4 are the radii of the circles at η = 0, 1/3, 2/3 and 1, respectively. The four geometric shape functions are given as

$$\begin{aligned} N_1 &= [27(1-\eta)^3 - 27(1-\eta)^2 + 6(1-\eta)]/6 \\ N_2 &= 9\eta[3(1-\eta)^2 - (1-\eta)]/2 \\ N_3 &= 9\eta(3\eta-1)(1-\eta)/2 \\ N_4 &= 3\eta(3\eta-1)(3\eta-2)/6 \end{aligned} \tag{26}$$

The various geometric parameters R_ϕ, R', R" , cos ϕ, sin ϕ, and $\partial\phi/\partial\eta$, etc. were defined in Ref. 11. Since, the coordinate ξ measures the subtending angle θ from the meridional axis, $\partial\theta/\partial\xi = 1$.

(b) Displacement Functions

The strain energy expression for a membrane shell can be written as

$$U = \frac{Eh}{2(1-\nu^2)} \int_A \left(\varepsilon_\phi^2 + \varepsilon_\theta^2 + 2\nu\varepsilon_\phi\varepsilon_\theta + \frac{1-\nu}{2}\varepsilon_{\phi\theta}^2\right) RR_\phi d\phi d\theta \tag{27}$$

where all the ε's are defined in Eq. 8. This strain energy expression

contains no derivative terms of w. Thus a linear function for w (with 3 constants) satisfies the interelement compatibility for w.

For the first type of triangular membrane element (21 d.o.f.'s), each vertex has 7 d.o.f.'s: u; $\partial u/\partial \xi$; $\partial u/\partial \eta$; v; $\partial v/\partial \xi$; $\partial v/\partial \eta$; and w. Either of the membrane displacement functions for u and v is a complete cubic polynomial in ξ and η with 10 constants. Two extra d.o.f.'s of u and v are added at the centroid of the element so that the 23 constants can be determined uniquely by the 23 d.o.f.'s. The two centroidal d.o.f.'s u and v are determined by writing them in terms of the rest of the d.o.f.'s.

For the second type of triangular membrane elements (39 d.o.f.'s), each vertex has 13 d.o.f.'s: w; u; $\partial u/\partial \xi$; $\partial u/\partial \eta$; $\partial^2 u/\partial \xi^2$; $\partial^2 u/\partial \xi \partial \eta$; $\partial^2 u/\partial \eta^2$, and the similar six for v. The membrane displacement functions for u and v are assumed the same as those by Dawe (32).

(c) Element Formulation

The formulation for the stiffness and mass matrices for the 21 d.o.f. triangular membrane element are obtained by using the numerical integration expressions in the forms similar to those shown within the summation signs in Eqs. 17 and 18, respectively. Within the triangular area, a total of 13 integration points were used. The area coordinates of these 13 points along with the corresponding weight factors are given in Ref. 33. The element formulation thus obtained is with reference to the local coordinates. It is finally transformed to that with reference to the global coordinates.

The formulative procedure for the 39 d.o.f. triangular membrane element is the same as that for the 21 d.o.f. element. The u and v displacement functions were assumed the same as those by Dawe (32) so that the $\partial u/\partial \eta$ and $\partial v/\partial \eta$ along the edge $\eta = 0$ are in the form of a cubic polynomial

in ξ. In addition, four constraints were imposed to ensure that the derivatives of u and v with respect to the axis normal to the other two edges also vary cubically along those edges.

(d) Evaluative Analysis

In order to evaluate the formulation for the 21 d.o.f. and the 39 d.o.f. triangular membrane elements, two examples were chosen.

(i) Axisymmetric Vibration of a Spherical Cap -- A spherical membrane and its geometric material parameters are shown in Fig. 9. Kraus (24) gave a solution of this problem using the shallow shell theory. It was assumed that the expression for the change in the curvature of the reference surface are identical to those of a flat circular plate. The resulting simplified differential equation is a Bessel's equation of first order. The natural frequencies for the present shell are given by the roots of the equation

$$J_1(\mu) = 0 \tag{28}$$

where $$\mu^2 = \frac{a^2\Omega^2}{R^2}(1+\nu)\frac{2-\Omega^2(1-\nu)}{(1-\Omega^2)} \tag{29}$$

and $$\Omega^2 = \frac{\rho\omega^2R^2}{E}$$

In the above equation a is the radius of the base circle of the spherical cap and is equal to 0.5R for the present case. R = 100 feet which is the radius of the sphere. The first five roots for μ in Eq. 28 are 3.832, 7.016, 10.17, 13.32, and 16.47. By substituting these values of μ into Eq. 29, one can obtain values of Ω^2 and hence ω, the natural frequency in rad/sec. For every value of μ, there are two values of ω. One of the value increases with μ without bound, whereas the other value

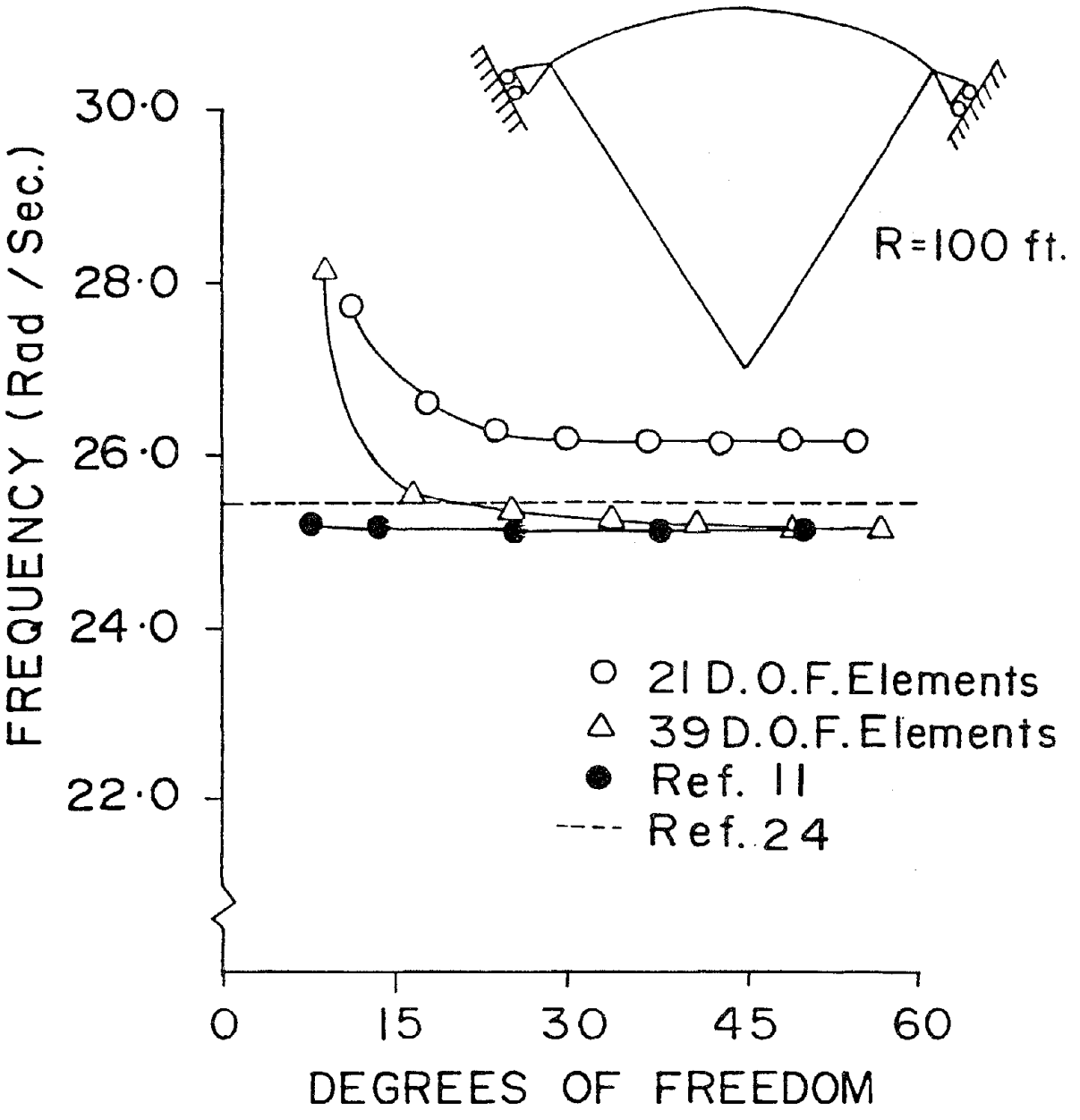

Figure 9 Axisymmetric Vibrations of a Spherical Membrane with a Subtending Angle of 60°, $E = 3 \times 10^7$ psf; $\nu = 0.3$; $\rho = 4.5$ lbs-sec^2/ft^4 (1 lb = 4.45 N, 1 ft = 0.305 m).

TABLE 3 - Natural Frequencies of Axisymmetric Modes of a Spherical Cap

Mode No	NATURAL FREQUENCY IN RAD/SEC			
	Lower value		Upper value	
(1)	Kraus (24) (2)	Present (3)	Kraus (24) (4)	Present (5)
1	25.44	25.15	210.4	197.8
2	25.70	25.62	381.4	357.2
3	25.77	25.73	551.7	515.2
4	25.79	25.78	721.9	674.2
5	25.80	25.81	892.2	835.5

is very close to and approaches a limiting value of $\sqrt{E/\rho}/R$. Five pairs of the natural frequency corresponding to the first five values of μ or the first five pair of modes are presented in Table 3. For each pair of modes, the distribution for the normal deflection w is the same but the distribution for the meridional displacement u is different.

When the present elements are used to solve the problem, only a small segment of the shell with a subtending angle of 5° at the apex was analyzed and both types of elements were used. The results for the natural frequency for the lowest axisymmetric mode are plotted against the number of d.o.f.'s using both types of elements. The converged values were obtained as 26.15 and 25.15 rad/sec. using the 21 and 39 d.o.f. elements, respectively. The alternative analytical solution given by Kraus (24) yields a value of 25.44 rad/sec. The results by using the quadrilateral membrane elements by Gran and Yang (11) were also plotted in Fig. 9, with a converged value of 25.15 rad/sec. The converged result obtained by using 39 d.o.f. triangular element is in good agreement with that obtained in Ref. 11.

The 39 d.o.f. element was thus used to obtain the natural frequencies corresponding to the first five pair of modes. The first five pairs of natural frequencies obtained using 19 such triangular elements (81 d.o.f.) are also given in Table 3. Agreement between the analytical and the present numerical results is good.

(ii) First Eccentric Frequency of a Fixed Based Cooling Tower -- The same fixed-base cooling tower analyzed in Table 2 was examined using the two types of triangular membrane elements. One half of the shell is modeled by using five different meshes (1x1, 2x2, 3x3, 4x4, and 5x5) for the 21 d.o.f. elements and four different meshes (1x2, 2x2, 2x3, and 3x3)

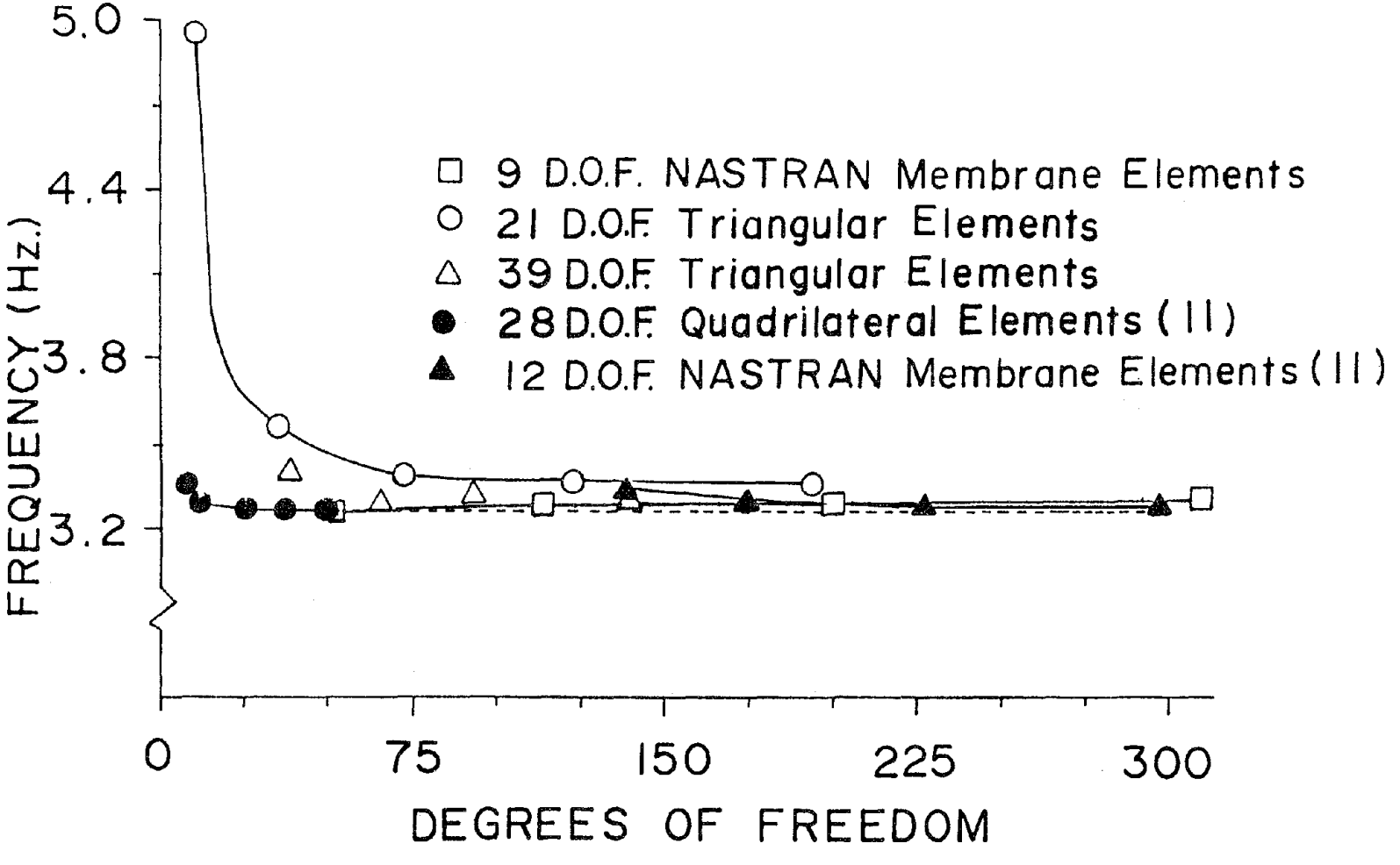

Figure 10 First Eccentric Natural Frequency of a Fixed Base Hyperbolic Cooling Tower Using the Two Types of Triangular Membrane Elements.

for the 39 d.o.f. elements. The results for the natural frequency for the first eccentric mode are plotted versus the number of d.o.f.'s in Fig. 10. The converged values obtained by using the 21 and 39 d.o.f. elements are 3.35 and 3.30 Hz, respectively. The results were also obtained by using the 9 d.o.f. triangular membrane plate elements of the NASTRAN Program. Four different mesh configurations (4x4, 6x6, 8x8 and 10x10) were employed to model one half of the shell. The results which converged to a value of 3.30 Hz are also shown in Fig. 10. The results by using the 12 d.o.f. quadrilateral membrane plate elements of the NASTRAN program and the 28 d.o.f. quadrilateral membrane shell elements (11) are also shown with the converged values being 3.28 and 3.27 Hz, respectively.

From the results obtained in Figs. 9 and 10, it is seen that both types of triangular membrane elements are reasonably accurate and efficient for use as filler elements in combination with the other two types of elements developed or suggested here. Since the 39 d.o.f. element contains the nodal derivative d.o.f.'s of $\partial^2 u/\partial \xi^2$, $\partial^2 u/\partial \eta^2$, $\partial^2 v/\partial \xi^2$ and $\partial^2 v/\partial \eta^2$, which the quadrilateral membrane elements (11) do not have, only the 21 d.o.f. elements were used in the following example where all types of elements were used.

CHAPTER 2

THREE ECCENTRIC FREQUENCIES OF A COLUMN-SUPPORTED COOLING TOWER USING THE WHOLE SET OF ELEMENTS

The cooling tower considered is defined by the following parameters: radius at the base of the shell = 182.25 ft. (55.58 m); radius at the throat = 116.5 ft. (35.5 m); radius at the top = 123 ft. (37.49 m); height of the shell excluding the columns = 449.75 ft. (137.08 m); height from the throat to the top of the shell 98.89 ft. (30.14 m); and thickness = 12 in. (0.305 m); modulus of elasticity = 4×10^6 psi (27.59 GN/m^2) Poisson's ratio = 0.167; mass density = 0.225×10^{-3} lbs-sec^2/in^4 (2.406×10^3 kg/m^3). The tower has 88 columns, each with the length of 41 ft. (12.5 m) and cross section of 24 in (0.61 m) by 52 in. (1.32 m) in the radial and circumferential directions, respectively. Each column inclines with the meridional line at an angle of $\pm$ 19°.

The modeling using the combination of the five types of elements is shown in Fig. 1. Only a quadrant of the cooling tower is modeled and the meshes for the five types of elements are shown in the figure.

The number of d.o.f.'s retained depends upon the boundary conditions which are dictated by the mode shapes considered. In this example, the three fundamental eccentric modes were considered. It had been shown that only these three modes are dominant in the earthquake response behavior of a cooling tower (29,7,9,10). For such modes, the model shown in Fig. 1 resulted in 412 d.o.f.'s. It is noted that if the general shell elements were used to model the entire shell height, a total of

641 d.o.f.'s would have to be used. Both lumped mass and consistent mass matrices were used. The results for the natural frequencies are given in Table 4.

This example was analyzed previously by Gould, Sen and Suryoutomo (7) using 14 doubly curved rotational shell elements and a column equivalent rotational shell element. It was also analyzed by Basu and Gould (8) using 11 doubly curved rotational shell elements and a modified open-type column equivalent rotational shell element. Both sets of results are shown in Table 4. It is seen that the agreements between the four sets of results are quite good except for that of the second eccentric mode using lumped mass model.

TABLE 4.-- Three Eccentric Natural Frequencies of a Column Supported Cooling Tower.

Longitudinal Mode Number m (1)	Circumferential Mode Number n (2)	NATURAL FREQUENCY IN HERTZS			
		Gould, Sen & Suryoutomo (Ref. 7) (3)	Basu and Gould (Ref. 8) (4)	Consistent Mass (5)	Lumped Mass (6)
1	1	2.296	2.336	2.333	2.284
	2	3.889	4.119	4.156	3.476
	3	7.730	7.056	6.952	6.885

CHAPTER 3

STATIC ANALYSIS OF A FIXED BASE COOLING TOWER DUE TO WIND LOAD

Wind loading is the most significant environmental loading to which a cooling tower is subjected to in its life span. Failure of the cooling towers at Ferrybridge (1) and Ardeer (2) led to various research programs towards the understanding of the nature of the wind loading (acting on the cooling tower) itself and the resulting structural response of the cooling towers. Billington and Abel (34) gave a reivew of the state-of-the-art of the design of the cooling towers subjected to wind loads. At present, the wind loading is essentially assumed to be quasi-static and is given by the following expression (35)

$$p = K_Z \, G \, q_{30} \, C_p(\theta) \tag{30}$$

where

p = effective velocity pressure in psf at height Z feet above the ground level;

K_Z = an exposure factor which determines the vertical profile of the wind due to the boundary layer effects of the ground and depends upon the terrain roughness;

G = gust response factor to take into account the dynamic response of the structure to turbulence;

$C_p(\theta)$ = a coefficient for the circumferential distribution of the wind pressure and is determined from the test results; and

$$q_{30} = 0.00256\ V_{f30}^2$$

is the basic velocity pressure in psf at 30 feet (9.15 m) above ground level obtained from the basic wind speed.

Abel and Billington (34) described these factors in great detail along with the methods to obtain them.

Although the wind loads are assumed to be quasi-static in the design, in reality, however, these loads are dynamic in nature. Furthermore, they are highly random in both time as well as in space. For proper understanding of the response of the cooling towers for the design purposes, the wind loads must be represented as accurately as possible and the theory of random vibrations must be used to account for the randomness of the wind loads.

For a given wind velocity V_o, the wind load effect P_w can be expressed as

$$P_w = W_S + W_D \tag{31}$$

where W_S = static wind effect due to mean wind velocity V; and

W_D = dynamic wind effect due to the fluctuating component V_o-V.

Based on the pressure distributions obtained directly from experimental measurements made on a full scale tower at Martin's Creek, Pa., a procedure to establish the level and distribution of the design dynamic wind pressure loading over a cooling tower, was given by Sollenberger, Scanlan and Billington (36).

Dynamic responses of the structure due to the fluctuating component were determined from a statistical response analysis (37, 38, 39) and

from a deterministic time history response analysis (36, 40, 41). Such responses have also been studied by measuring aeroelastic models in wind tunnels (42, 43) and by measuring a full scale prototype (43).

The static response of the cooling tower due to the mean wind velocity can be determined by analyzing the cooling tower subjected to a basic pressure given by Eq. 30 with G = 1. In this study, the static response of a cooling tower subjected to a given pressure distribution is determined. The cooling tower under consideration is the same as that analyzed for natural frequencies in Table 2. This tower was previously analyzed by Albasiny and Martin (44) using finite difference method and by Chan and Firmin (45) using rotational-type shell finite element of the SABA family. Gould and Sen (46) developed and used a refined mixed method rotational type shell element to study the static response due to the wind loads. In all the above studies, the circumferential distribution of the pressure coefficient was assumed to be given by the Batch and Hopley distribution (44). This distribution, including a 0.5 internal suction, is given by

$$
\begin{aligned}
C_p(\theta) &= -1.524 \cos(1.89\,\theta) && \text{for } 0^\circ \le \theta \le 47.6 \\
&= 0.69 \sin[3.61\,(\theta - 47.6)] && \text{for } 47.6 < \theta \le 100^\circ \\
&= -0.21 && \text{for } 100^\circ < \theta \le 180^\circ
\end{aligned}
\qquad (32)
$$

The distribution is shown in Fig. 11. In all the above studies the pressure distribution was approximately represented by a ten term Fourier Cosine series. For the present 48 d.o.f. general shell element, such a decomposition is not necessary.

The vertical profile of the wind velocity is assumed to be constant throughout the shell height ($K_Z = 1$) and the value of $q(=\frac{1}{2}\rho V^2)$ is assumed

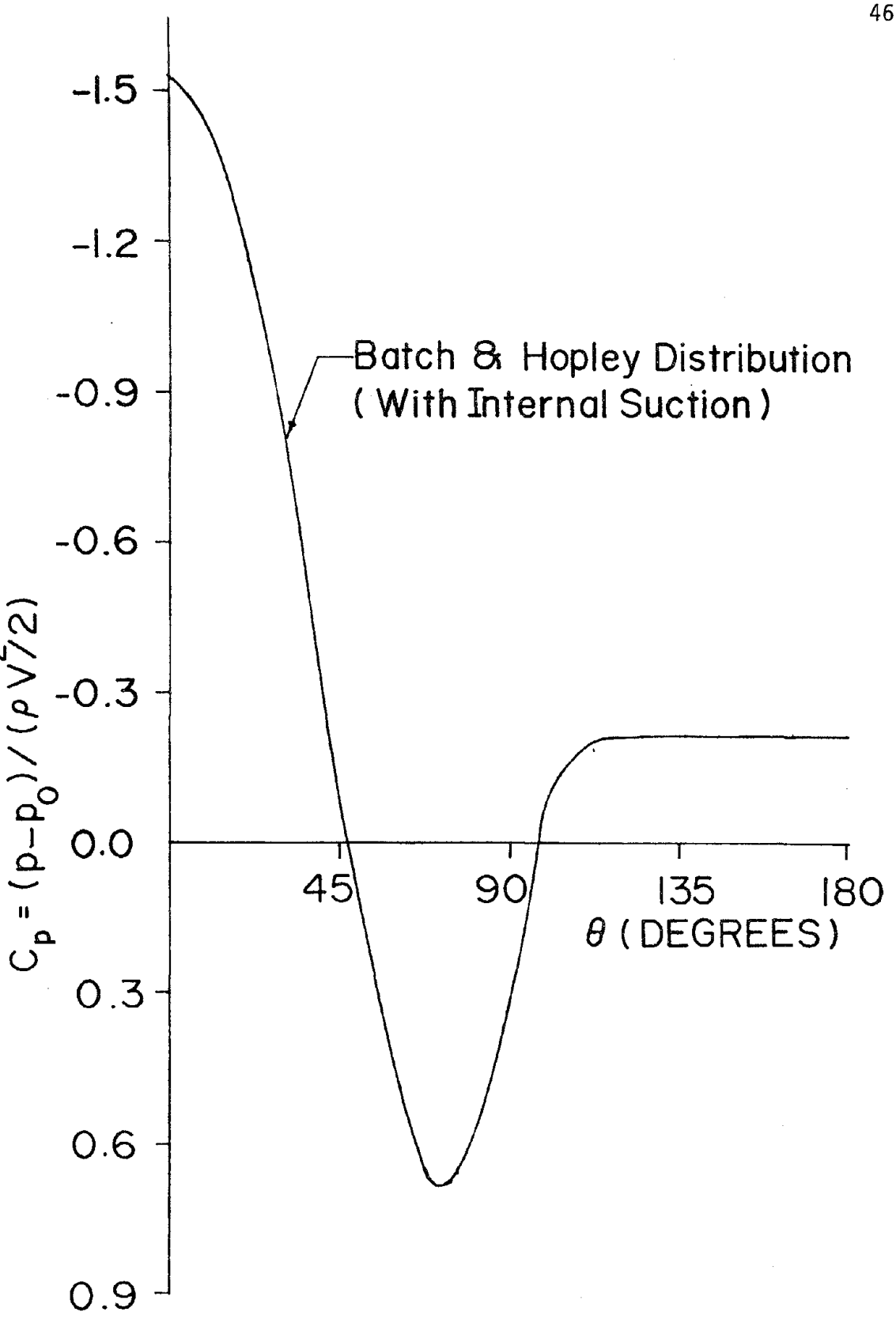

Figure 11 Pressure Distribution Around the Circumference. (With Internal Suction C_p = 0.5).

to be 1 psf corresponding to V = 19.76 MPH.

Three different mesh configurations using the present 48 d.o.f. general shell elements (4x4, 5x5, and 6x6) were used to model one half of the shell. Since the wind loading was assumed to be symmetric, it suffices to model only one half of the shell. But if the pressure distribution is not symmetric, as may be the case on an actual cooling tower, the entire shell has to be modeled. In each of the meshes employed, the elements at the base of the tower were of a height 1.8% of that of the cooling tower. Elements of such a small shell height were necessary to properly capture the abrupt variation of the meridional moment at the base. The topmost elements in all the meshes were of a height 18.2% of the shell height. Each element subtended equal angle in the circumferential direction. The pressure loads were converted into the nodal loads using consistent load vector. The results for the maximum meridional stress resultant N_ϕ at $\theta = 0°$ as obtained in the present analysis for three meshes are given in Fig. 12. It should be mentioned that the meridional stress resultant should be determined as accurately as possible because the amount of steel reinforcement in the shell is dependent upon this resultant. Fig. 13 gives the variation of the meridional bending moment along the shell height. The bending moment is negligible throughout the shell height except for a narrow zone at the base. In both figures, the results obtained by Gould and Sen (46) using a total of 19 rotational-type shell elements are also shown. Excellent agreement between the two sets of results is seen.

Variation of the maximum radial displacement at $\theta = 0°$ along the shell height is given in Fig. 14. Results obtained by Chan and Firmin (45) are also shown. These results are obtained for a shell thickness

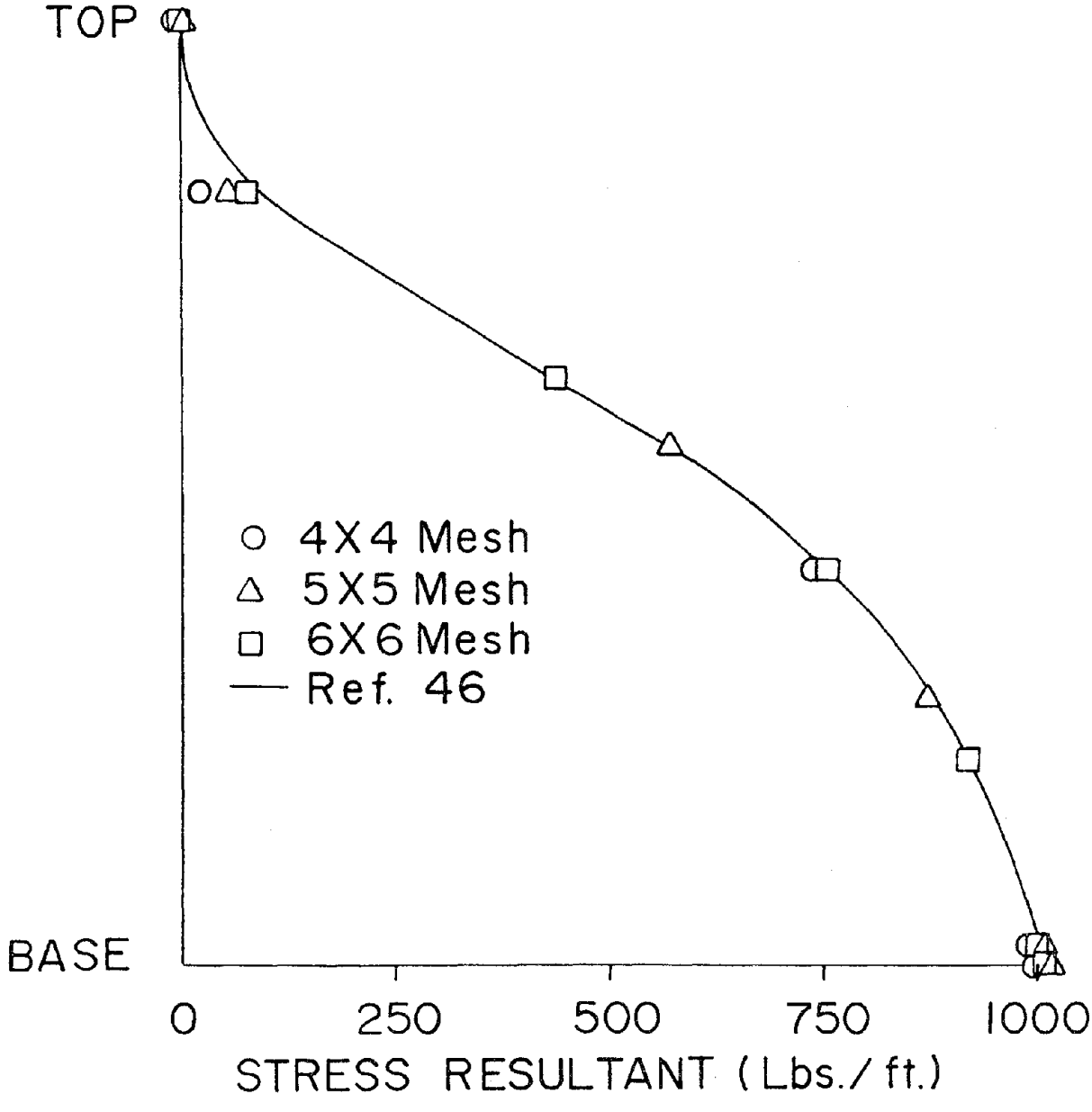

Figure 12 Meridional Stress Resultant (N_ϕ) Due to Wind Load. ($\rho V^2/2$ = 1 psf; 1 lb = 4.5 N, 1 ft. = 0.305 m).

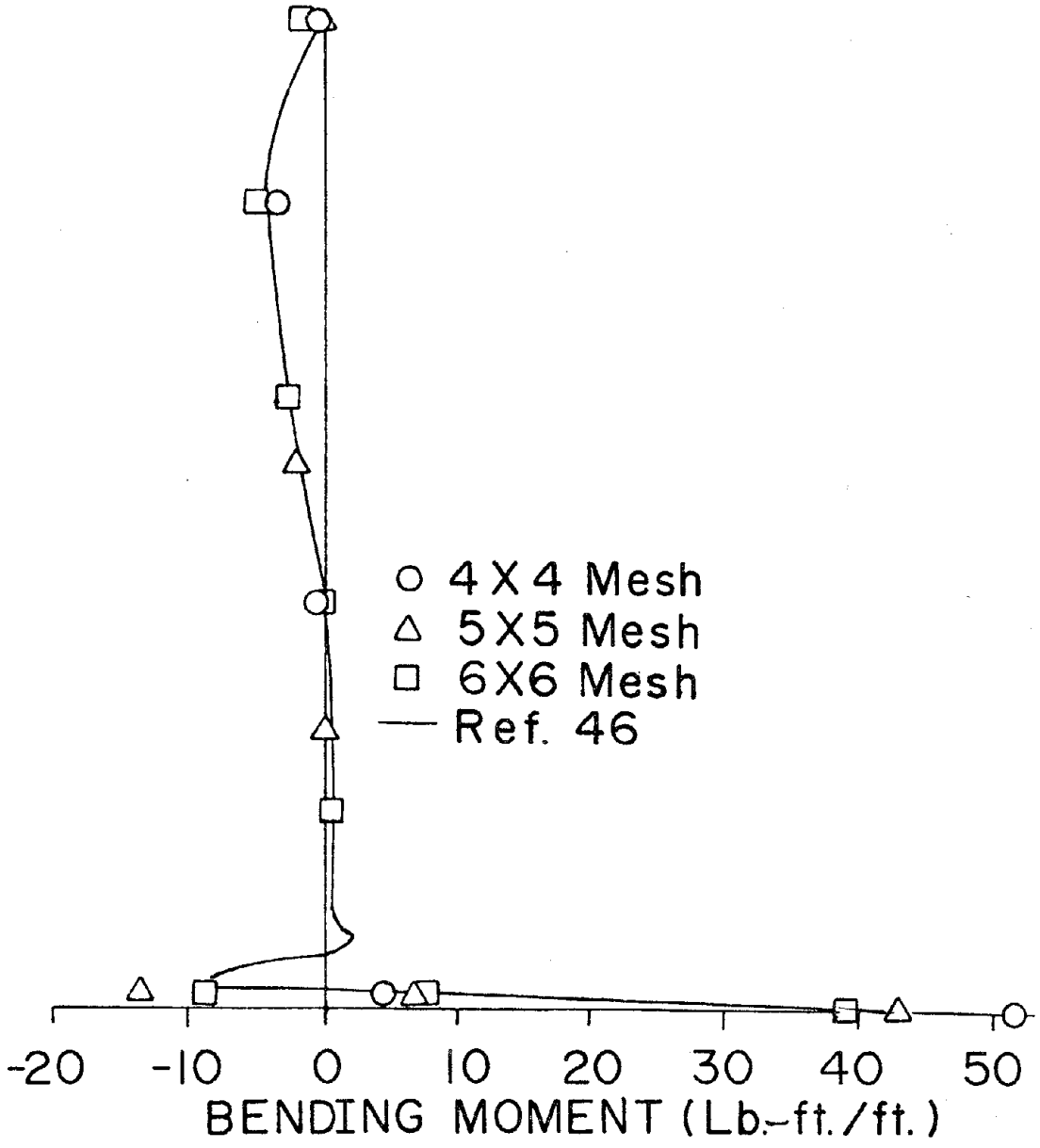

Figure 13 Meridional Bending Moment (M_ϕ) Due to Wind Load ($\rho V^2/2$ = 1 psf; 1 lb. = 4.5N; 1 ft. = 0.305m).

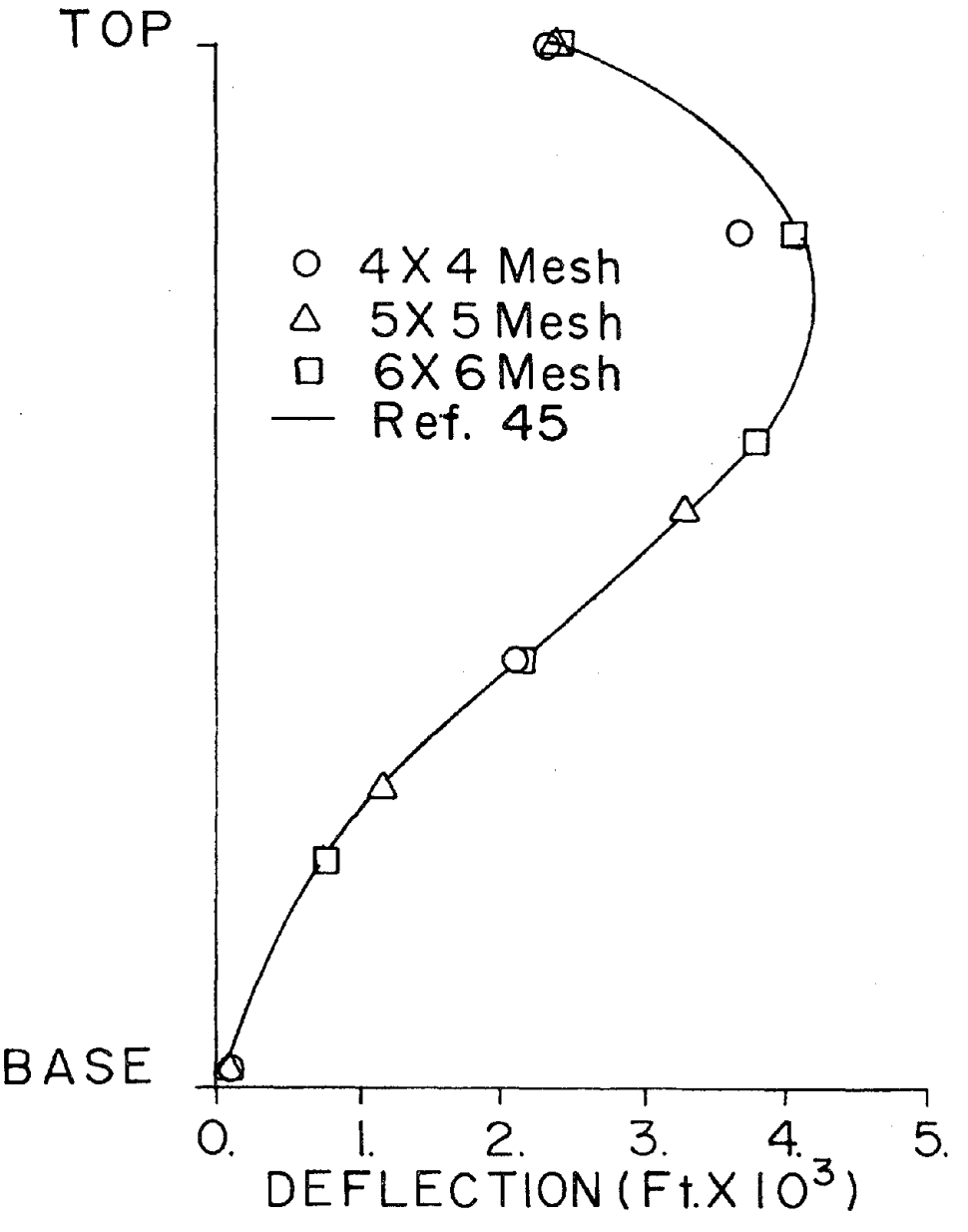

Figure 14 Radial Deflection at $\theta = 0$ Due to Wind Load. ($\rho V^2/2$ = 1 psf; thickness = 7 in.; 1 lb. = 4.5N, 1 ft. = 0.305m.)

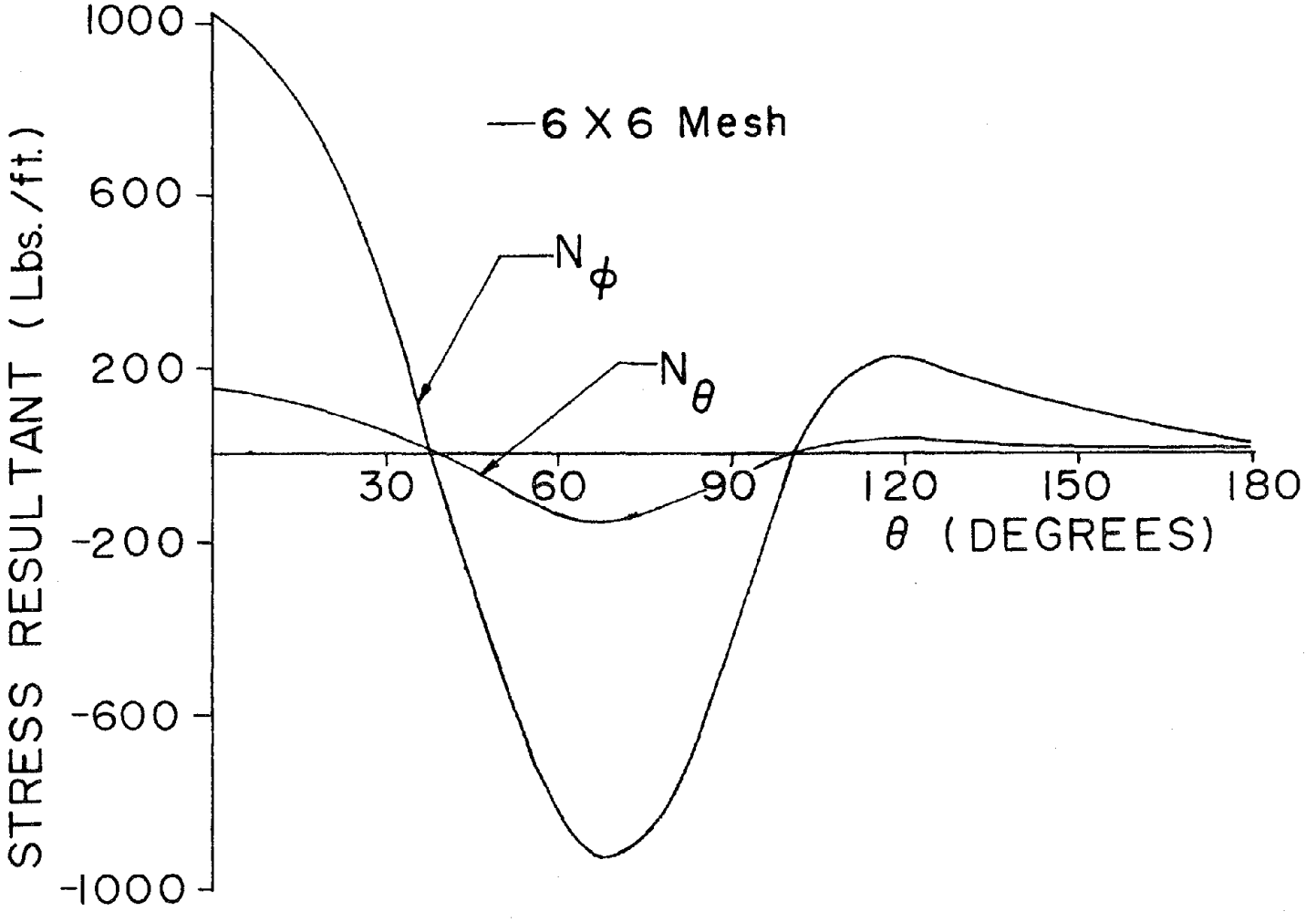

Figure 15 Distribution of Membrane Stress Resultants N_ϕ and N_θ at the Shell Base Due to Wind Load ($\rho V^2/2$ = 1 psf, 1 lb = 4.5 N; 1 ft = 0.305 m).

of 7 in. (17.78 cm) rather than the shell thickness of 5 in. used in the determination of the stresses. Once again excellent agreement is seen.

Figure 15 shows the variation of the membrane stress resultants in the circumferential direction at the base of the shell obtained using 6x6 mesh for half of the shell. This distribution is quite similar to the pressure distribution shown in Fig. 11. The maximum tensile stress which occurs at the windward meridian ($\theta = 0°$) is larger than the maximum. compressive stress occurring at about 70° from the windward meridian.

From the above results, it can be concluded that the response of the cooling tower can be accurately predicted using the present developments if the wind loads are assumed as quasi-static and known. Although the results are obtained for a pressure distribution which is symmetric about the direction of wind and is uniform along the shell height, the results for non-symmetric and non-uniform pressure loads can be determined just the same.

CHAPTER 4

CONCLUDING REMARKS

In this study, a set of shell elements, with a capability to investigate the stability and dynamic response of complex thin shell structures, has been formulated. A computer program has been developed and evaluated by solving a series of examples pertaining to shells of revolution. The above set was developed with a view to adequately model and analyze column-supported cooling towers subjected to wind and earthquake loadings in an optimal fashion.

It has been learned from previous studies of some examples of seismic response of column-supported cooling towers (9, 10) that the cooling tower shell behaves primarily as a membrane. The only appreciable bending is confined to a narrow band at the shell base. It has also been learned that only the eccentric modes (n=1) are responsive to seismic disturbances (29, 7, 9, 10).

As a first step to accurately and efficiently model the membrane portion of such shells, a high-order doubly curved quadrilateral membrane element was developed by Gran and Yang (11). With the intent to optimize the finite element modeling of a column supported cooling tower for seismic response analysis and with the intent to model each column discretely, a family of finite elements as depicted in Fig. 1 has been adopted, modified, or extended in this study: (1) a 16 d.o.f. column element; (2) a 48 d.o.f. doubly-curved quadrilateral general shell element: (3) a 42 d.o.f. doubly-curved quadrilateral general-membrane transition element; (4) a 21

d.o.f. and a 39 d.o.f. doubly-curved triangular membrane filler element; and (5) a 28 d.o.f. doubly-curved quadrilateral membrane element.

Element (1) is a 3-D variation of that of Ref. 13. Element (2) is the one that was developed in Ref. 12 but with some difference in formulative procedures and with extensive application in this study to the cooling tower analysis of buckling and vibration with initial stresses. Element (3) is developed here. Elements (4) are the modified version of those in Refs. 30 and 31 to fit the present need. Element (5) is adopted from Ref. 11. Various examples have been demonstrated to evaluate an individual type, a few combined types, and the whole set of elements and the results are all quite good.

During a seismic disturbance, the regions containing the joints between the columns and the base of the shell are vulnerable and it is highly desirable that the state of the stress distributions in these regions at certain critical moments be studied and understood. It is also highly desirable that material nonlinearity be considered in such a study. For these purposes, the modeling of the base regions by using the discrete column elements and quadrilateral general shell elements is suggested.

Research is now being carried out to study the nonlinear stress distribution in a cooling tower subjected to seismic disturbances. The effect of wind loads is also being studied. As a first step, the response of the cooling tower due to the mean wind velocity has already been studied and the results obtained are in excellent agreement with the alternatively available results. The cooling tower response due to the fluctuating velocity component will be studied in collaboration with Professor Y.K. Lin using the theory of random vibrations. For wind disturbances, the breathing modes such as $n = 6$ are also important. For

breathing modes with circumferential wave numbers equal to 4 or 5, or above, the shell no longer behaves primarily as a membrane. The present general shell elements must be used through the shell structure.

In addition to the adequate representation of the structural properties (mass, stiffness and damping) of the cooling tower, the characteristics of the wind loading (spectral characteristics of the gust, spatial distribution and correlation of pressure over the tower surface etc.) must be accurately known. Efforts are now underway, under the direction of Professor Anshel L. Schiff to determine the wind loads by performing measurements on a full scale cooling tower. The dynamic response will also be measured to corroborate the results with those obtained theoretically.

REFERENCES

1. "Report of the Committee of Inquiry into the Collapse of the Cooling Tower at Ferrybridge, Monday, Nov. 1, 1965," Central Electricity Generating Board, Her Majesty's Stationary Office, London, England, 1966.

2. Miller, K.A.G. (chairman), "Report of the Committee of Inquiry into the Collapse of the Cooling Tower at Ardeer Nylon Works, Ayrshire on Thursday, 27th September 1973," Imperical Chemical Industries Limited, Petrochemicals Division, available from Engineering Services Department, Imperical Chemical House, Millbank, London SWIP 3JF, no date.

3. Carter, R.L., Robinson, A.R., and Schnobrich, W.C., "Free Vibration of Hyperbolidal Shells of Revolution," Journal of the Engineering Mechanics Division, ASCE, Vol. 95, No. EM5, Proc. Paper 6808, Oct. 1969, pp. 1033-1052.

4. Hashish, M.G., and Abu-Sitta, S.H., "Free Vibration of Hyperbolic Cooling Towers," Journal of the Engineering Mechanics Division, ASCE, Vol. 97, No. EM2, Proc. Paper 8037, Apr., 1971, pp. 253-269.

5. Sen, S.K., and Gould, P.L., "Free Vibration of Shells of Revolution Using FEM," Journal of the Engineering Mechanics Division, ASCE, Vol. 100, No. EM2, Proc. Paper 10488, April, 1974, pp. 283-303.

6. Nelson, R.L., "Free Vibration Analysis of Cooling Towers," Shock and Vibration Digest, Vol. 12, No. 12, Dec., 1980, pp. 15-24.

7. Gould, P.L., Sen, S.K., and Suryoutomo, H., "Dynamic Analysis of Column-Supported Hyperboloidal Shells," Earthquake Engineering and Structural Dynamics, Vol. 2, 1974, pp. 269-279.

8. Basu, P.K., and Gould, P.L., "Finite Element Discretization of Open-Type Axisymmetric Elements," International Journal for Numerical Methods in Engineering, Vol. 14, No. 2, 1979, pp. 159-178.

9. Gran, C.S., and Yang, T.Y., "NASTRAN AND SAP IV Applications on the Seismic Response of Column-Supported Cooling Towers," Journal of Computers and Structures, Vol. 8, No. 6, June, 1978, pp. 761-768.

10. Gran, C.S., and Yang, T.Y., "Refined Analysis of the Seismic Response of Column Suported Cooling Towers," Journal of Computers and Structures, Vol. 11, No. 3, 1980, pp. 225-231.

11. Gran, C.S., and Yang, T.Y., "Doubly Curved Membrane Shell Finite Element," Journal of the Engineering Mechanics Division, ASCE, Vol. 105, No. EM4, Proc. Paper 14741, Aug., 1979, pp. 567-584.

12. Fonder, G.A., "Studies in Doubly Curved Elements for Shells of Revolution," Finite Elements for Thin Shells and Curved Members, D.G. Ashwell and R.H. Gallagher, ed., John Wiley and Sons, Inc., New York, N.Y., 1976, pp. 113-129.

13. Yang, T.Y., and Sun, C.T., "Finite Elements for the Vibration of Framed Shear Walls," Journal of Sound and Vibration, Vol. 27, No. 3, 1973, pp. 297-311.

14. Ashwell, D.G., and Gallagher, R.H., ed., Finite Elements for Thin Shells and Curved Members, John Wiley and Sons, Inc., New York, N.Y., 1976.

15. Gallagher, R.H., "The Development and Evaluation of Matrix Methods for Thin Shell Structural Analysis," Report No. 8500-902011, Bell Aerosystems, Buffalo, N.Y., June 1966.

16. Cantin, G., and Clough, R.W., "A Curved Cylindrical-Shell Finite Element," AIAA Journal, American Institute of Aeronautics and Astronautics, Vol. 6, No. 6, June 1968, pp. 1057-1062.

17. Bogner, F.K., Fox, R.L. and Schmit, L.A.,Jr., "A Cylindrical Shell Discrete Element," AIAA Journal, American Institute of Aeronautics and Astronautics, Vol. 5, No. 4, Apr., 1967, pp. 745-750.

18. Greene, B.E., Jones, R.E., McLay, R.W., and Strome, D.R., "Dynamic Analysis of Shells Using Doubly-Curved Finite Elements," Proceedings of the 2nd Conference on Matrix Methods in Structural Mechanics, Air Force Flight Dynamics Laboratory, TR-68-150, Dayton, Ohio, Dec. 1969, pp. 185-212.

19. Yang, T.Y., "High Order Rectangular Shallow Shell Finite Element," Journal of the Engineering Mechanics Division, ASCE, Vol. 99, No. EM1, Proc. Paper 9519, Feb. 1973, pp. 157-181.

20. Novozhilov, V.V., Thin Shell Theory, 2nd ed., Wolters-Noordhoff Publishing, Groningen, The Netherlands, 1970, pp. 22-23.

21. Gallagher, R.H., and Yang, T.Y., "Elastic Instability Predictions for Doubly-Curved Shells," Proceedings of the 2nd Conference on Matrix Methods in Structural Mechanics, TR-68-150, Dec. 1969, Air Force Flight Dynamics Lab., Dayton, Ohio, Dec., 1969, pp. 711-739.

22. Larsen, P., "Large Displacement Analysis of Shells of Revolution Including Creep, Plasticity and Viscoelasticty," thesis presented to the University of California at Berkeley, Calif., in 1972, in partial fulfillment of the requirements for the degree of Doctor of Philosophy.

23. Fonder, G.A., and Clough, R.W., "Explicit Addition of Rigid-Body Motions in Curved Finite Elements," AIAA Journal, American Institute of Aeronautics and Astronautics, Vol. 11, No. 3, Mar., 1973, pp. 305-312.

24. Kraus, H., Thin Elastic Shells, John Wiley and Sons, Inc., New York, N.Y., 1967, pp. 136-140, 316-319.

25. Kalnins, A., "Effect of Bending on Vibrations of Spherical Shells," The Journal of the Acoustical Society of America, Vol. 36, No. 1, Jan., 1966, pp. 74-81.

26. Zarghamee, M.S., and Robinson, A.R., "A Numerical Method for Analysis of Free Vibration of Spherical Shells," AIAA Journal, American Institute of Aeronautics and Astronautics, Vol. 5, No. 7, July 1967, pp. 1256-1261.

27. Brush, D.O., and Almroth, B.O., Buckling of Bars, Plates and Shells, McGraw-Hill Book Company, 1975, pp. 167-168.

28. Deb Nath, J.M., "Free Vibration, Stability and Nonclassical Modes of Cooling Tower Shells," Journal of Sound and Vibration, Vol. 33, No. 1, 1974, pp. 79-101.

29. Abu-Sitta, S.H. and Davenport, A.G., "Earthquake Design of Cooling Towers," Journal of the Structural Division, ASCE, Vol. 96, No. ST9, Proc. Paper 7524, Sept., 1970, pp. 1889-1902.

30. Cowper, G.R., Lindberg, G.M., and Olson, M.D., "A Shallow Shell Finite Element of Triangular Shape," International Journal of Solids and Structures, Vol. 6, 1970, pp. 1133-1156.

31. Thomas, G.R., and Gallagher, R.H., "A Triangular Shell Finite Element: Linear Analysis," NASA C.R. 2482, July, 1975.

32. Dawe, D.J., "High-Order Triangular Finite Element for Shell Analysis," International Journal of Solids and Structures, Vol. 6, 1975, pp. 1097-1110.

33. Strang, G., and Fix, G.J., An Analysis of the Finite Element Method, Prentice Hall, 1973, pp. 156-163.

34. Billington, D.P., and Abel, J.F., "Design of Cooling Towers for Wind," Proceedings of the Speciality Conference on Methods of Structural Analysis, University of Wisconsin-Madison, Aug., 22-25, 1976, pp. 242-267.

35. "Reinforced Concrete Cooling Tower Shells: Practice and Commentary," Report of the ACI-ASCE Committee 334, February, 1976.

36. Sollenberger, N.J., Scanlan, R.H., and Billington, D.P., "Wind Loading and Response of Cooling Towers," Journal of the Structural Division, ASCE, Vol. 106, No. ST3, March 1980, pp. 601-621.

37. Abu-sitta, S.H., and Hashish, M.G., "Dynamic Wind Stresses in Hyperbolic Cooling Towers," Journal of the Structural Division, ASCE, Vol. 99, No. ST9, Sept., 1973, pp. 1823-1835.

38. Hashish, M.G., and Abu-sitta, S.H., "Response of Hyperbolic Cooling Tower to Turbulent Wind," Journal of the Structural Division, ASCE, Vol. 100, No. ST5, May, 1974, pp. 1037-1051.

39. Singh, M.P., and Gupta, A.K., "Gust Factors for Hyperbolic Cooling Towers," Journal of the Structural Division, ASCE, Vol. 102, No. ST2, Feb., 1976, pp. 371-386.

40. Steinmetz, R.L., Billington, D.P., and Abel, J.F., "Hyperbolic Cooling Tower Dynamic Response to Wind," Journal of the Structural Division, ASCE, Vol. 104, No. ST1, Jan., 1978, pp. 35-53.

41. Basu, P.K., and Gould, P.L., "Cooling Towers Using Measured Wind Data," Journal of the Structural Division," ASCE, Vol. 106, No. ST3, March 1980, pp. 579-600.

42. Armitt, J., "Wind Loading on Cooling Towers," Journal of the Structural Division, ASCE, Vol. 106, No. ST3, March 1980, pp. 623-641.

43. Niemann, H.-J., and Ruhwedel, J., "Full-Scale and Model Tests on Wind-Induced, Static and Dynamic Stresses in Cooling Tower Shells," Engineering Structures, Vol. 2, April 1980, pp. 81-89.

44. Albasiny, E.L., and Martin, D.W., "Bending and Membrane Equilibrium in Cooling Towers," Journal of the Engineering Mechanics Division, ASCE. Vol. 93, No. EM3, June 1967, pp. 1-17.

45. Chan, A.S.L., and Firmin, A., "The Analysis of Cooling Towers by the Matrix Finite Element Method. Part I: Small Displacements," The Aeronautical Journal of the Royal Aeronautical Society, Vol. 74, No. 10, London, England, Oct. 1970, pp. 826-835.

46. Gould, P.L., and Sen, S.K., "Refined Mixed Method Finite Elements for Shells of Revolution," Proceedings of the Third Conference on Matrix Methods in Structural Mechanics, Air Force Flight Dynamics Lab., TR-71-160, Dayton Ohio, Dec. 1973, pp. 397-421.